

Dear editor and referees,

We were grateful to receive the very constructive reviews of our paper “The GEOVIDE cruise in May-June 2014 reveals an intense Meridional Overturning Circulation over a cold and fresh subpolar North Atlantic”. Thank you very much to the 3 anonymous referees. We will incorporate in the manuscript the majority of their comments and we think the scientific results will be better exposed than in the first submission. Before dealing with the referee comments in detail, we wrote an answer to a concern that is common to the three reviews: the misunderstanding about the timescales dominating the cooling and freshening of the subpolar North Atlantic. Following, we answer point by point each comment of the three referees.

One result of our paper is the co-existence in May – June 2014 of the cooler and fresher eastern subpolar North Atlantic (SPNA) in relation to the mean 2002 – 2012, and the relative intense Meridional Overturning Circulation and heat transport across the OVIDE section. In the region delimited by 40°N – 60°N, 45°W – 10°W, the evolution of both (i) ocean heat and freshwater content in the upper 1000 m and (ii) air-sea fluxes of heat and freshwater since 2013 reveals that the atmospheric forcing is mostly responsible for the strong TS anomalies of 2014. However, as pointed by the three reviewers, we did not discuss the decadal context of our observations and missed to refer to Robson et al. (2016; 2017) who identified a new cooling period in the subpolar North Atlantic starting in mid-2000, a cooling period affecting at decadal time-scale.

In our revision, we will include a new figure showing the evolution of heat content in the upper 1000m of the region 40°N – 60°N, 45°W – 10°W (see Figure 1 in this document). Based on this figure, that shows a long term heat content decrease starting in the mid-2000s, we will be able to illustrate Robson et al. (2016; 2017). We also observe intensification in heat content decrease from 2013 to 2014, just the episode we discuss in our paper. Thus, the 2013-2014 cooling episode is inserted in the cooling at longer period of time detected by Robson et al. (2016; 2017). We show in our paper that the former was dominantly produced by the local atmospheric forcing over the 2013-2014 winter. Our results are in agreement with a recent paper, Frajka-Williams et al., (2017, in Scientific Reports): they exposed that the rapid cooling registered between 2013 and 2015 in the subpolar North Atlantic was explained by the atmospheric forcing since the effects of a MOC slow-down at 26°N is too slow to explain the observed rapid cooling.

Following this explanation, the third paragraph of the introduction will be restructured and the references to Robson et al. (2016-2017) added. The discussion 4.2 will also be expanded in order to place our observations in the context of a longer time scale. The figure 1 in this document will be inserted in the new ms.

We copied the referee comments in this document in blue font followed by our answers in black font.

Anonymous Referee #1

Received and published: 15 August 2017

One of the main findings in this paper is that despite the ongoing cooling/freshening anomaly in the SPNA, the authors measure stronger heat transport across the OVIDE section during the GEOVIDE cruise in May-June 2014. The authors further conclude by strongly stating that air-sea (heat and freshwater) fluxes were the dominant factor for the observed changes and that ocean circulation played a minor role.

The authors seem to have ignored the fact that the subpolar gyre (SPG) cooling/freshening is part of a decadal trend most likely initiated by ocean advection and circulation. There are evidence that the SPG temperature and salinity reversed already in 2005 (e.g. Robson et al. 2016, Nature Geoscience), and that the NAO shifted more to the positive state later on around 2011. The 2014 cooling/freshening thus may have been enhanced by air-sea fluxes (not locally formed), but it is important to keep in mind that the cooling as well as the freshening did not start in 2014 as the authors mention. It was well underway!

Nevertheless, I think the paper is good and taking into account what I have mentioned above as well as my comments below will help improve the paper, which I recommend for publication after these issues have been resolved.

Major comments

I think the authors need to focus on the 2014 event as being part of the (multi-)decadal cooling/freshening rather than the instigator of it. A robust discussion along these lines is therefore strongly recommended.

Yes, we agree that the 2014 event was not the instigator; it appears to add to the decadal cooling started in 2005 and linked by Robson et al. (2016; 2017) to ocean circulation and heat transport. This point will be clarified in the discussion.

Furthermore, I wonder also how the authors reconcile the fact that there are numerous studies (see e.g. Robson et al. 2017, Clim Dyn, and references therein) demonstrating that the western SPG is dominated by surface fluxes, while the eastern SPG is dominated by ocean advection.

We agree with the reviewer this applies on the decadal time scales. Our study focuses on an inter-annual event dominantly forced by local air-sea fluxes that appears to add to the decadal signal.

How do you explain the large-scale salinity anomaly in Fig. 8 that spans both the SPNA and the region of the Gulf Stream? there is very little discussed about this basin-scale feature.

Your comment is very interesting and further investigations in the Gulf Stream region would be necessary to determine whether it is a coherent basin-scale feature especially because the negative salinity anomaly is associated with a positive temperature anomaly in the Gulf Stream Region but to a negative temperature anomaly in the SPNA. Our objective is to understand what was observed during the cruise in 2014. In order to interpret the large-scale salinity anomaly, we estimated the freshwater content change in the box 40°N – 60°N, 45°W – 10°W using the ISAS data shown on Figure 8, data from other data sources (EN4 and JAMSTEC), as well as air-sea freshwater flux (ERA-interim and NCEP), see Figure 10 in the initial ms. The surface freshwater fluxes in the eastern SPNA were found to be important in the observed salinity anomaly.

Comments

I think the calculations and results are straightforward, but I have some comments that can help to further improve the paper: Using the inverse model the authors and thereby identify all main flows, and show that the ship-ADCP velocities are largely similar, at least in structure, to those based on the inverse modelling. I suggest to compare your transport numbers, whenever possible, to other studies for a complete picture.

We understand your suggestion. In fact, comparing transport numbers with previous studies was extensively done by Daniault et al. (2016), D2016 hereafter, who described the mean state of the circulation in the SPNA based on OVIDE data and the existing literature (e.g. Rossler et al. (2015), Sarafanov et al. (2008; 2012), Väge et al. (2008; 2011)). In this study, we only compare with results in other works when significant differences with D2016 were found (for example Väge et al., 2011).

Weaker NAC during 2014 is an interesting finding. The top-to-bottom transport of $0 \pm 6\text{Sv}$ as compared to the $11 \pm 4\text{ Sv}$ estimated by D2016 is large. I believe it is possible to show this large-scale shift from altimetry along the eddy-blockage and the doubling of the intensity of the SAF, which the authors are briefly mentioning in lines 404-412. Please elaborate also on the transfer of transport from the northern to the central branch, it is not clear to me how this occur!

We found your idea very good, and we plotted the mean ADT contours for 2002-2012 and for 2014 after removing the trend in the sea-level rise (2.8mm/yr in our region), see Fig. 2 and 3, respectively, in this document. The colors show the current velocity and highlight the energetic areas. Then we plotted the stream lines encompassing the SAF in bold; they have the same ADT values in both figures (Fig 2. and Fig. 3 in this document) and represent a slope of 15 cm in the ADT. We also plotted in both figures a red circle at the 2014 SAF position (station 26 of GEOVIDE). To interpret this figure, we assume that the bold streamlines delimit the travel of the surface waters crossing the OVIDE section at the SAF position. For comparison, we added in Fig. 3 the 2002 – 2012 mean stream lines encompassing the SAF in red. We see that along the OVIDE section, the SAF is quite narrow and located more to the southeast in 2014, when compared to the 2002-2012 mean. But more important, the NAC transport seems to be dispatched on a larger area in the mean, encompassing the permanent eddy characteristic of the northern branch of the NAC. So in the mean, the NAC transport is shared among both branches, while in 2014, it is concentrated in the SAF. Finally, note that those lines end up at the same position between Iceland and Scotland, so in both cases, the surface water included in the SAF (as defined here) feeds the Atlantic inflow to the Nordic Seas.

To conclude, it seems that we were wrong in suggesting an eddy blocking of the northern branch. We now see that the frontal zone moved to the south, leaving no transport for the northern branch identified during the previous decade.

Note that Fig. 2 will not be included in the new ms.

Furthermore, as the authors mention (lines 520-527), they expected an expansion of the SPG. Could you better discuss what the displacement of the SAF actually means?

We agree that this subject requires more discussion, so we will displace the part of the last paragraph of the discussion about the expansion of the SPG to the fourth paragraph of the discussion where we indicated the southeastward displacement of the SAF in 2014. There, we will better explain that the “displacement of the SAF” is the southeastward displacement of the front along the OVIDE section in 2014 as compared with the 2002-2012 average. In fact, Bersch et al. (2002) interpreted that in the eastern SPNA, during the warming period from

mid-1990s, there was a northwestward displacement of the SAF coinciding with a contraction of the SPNA. Following Bersch et al. 2002, we proposed that the SAF southeastward displacement suggests a new expansion of the SPNA, consistently with the persistently positive winter NAO index since 2011 (except in 2012). However, both the meandering of the NAC in the eastern SPNA and the lack of distance in time make difficult a strong assessment involving decadal variability as in Bersch et al. (2002).

The green box in Fig. 9 seems very large to me to be considered as the eastern North Atlantic. It is rather peculiar that in the net freshwater field you are averaging over an area that almost symmetrically includes positive and negative net FW.

Surely, the referee is right and the box is somehow large to name it the “eastern subpolar North Atlantic”. However, our intention was to define a box containing the whole OVIDE section, including upstream and downstream anomalies. We were also greatly surprised when we saw the almost symmetrically pattern of the air-sea freshwater flux, with the OVIDE section as the diagonal of the green box separating the negative and positive net FW. It is actually an interesting subject for our future research. It necessarily has a physical explanation, but it can also be fortuitous. In spite of the symmetry, the integrated net FW is positive, which is in agreement with the fact that the eastern SPNA is getting fresher. Diminishing the box (to the northeast) reinforces our conclusion.

The eddy part of the paper is clear, although full of details, it completes the picture well. It is however not easy from a visualization point view to see the eddies and the colors in the figure. Suggest to improve this and make it as clear as possible to the readers, perhaps similar to Fig. 6 of D2016.

We understand your concern. We did different figures representing AVISO information (ADT, and surface velocity) when preparing the first version of the manuscript, and we thought that the representation we propose is more intuitive for our colleagues in biogeochemistry who are interested in the velocity information. We plotted the same way than D2016 but even if the eddies are visible, reading the ADT contours requires some skills typical of the physical community. Therefore, we prefer to keep our presentation, but, to guide the reader, we will introduce more information about the colors of the squares in the next version of the ms.

Consider adding a reference to a recent paper by Rossby et al. (2017, JGR) on the fluxes across 59.5N. Their MOC transport estimate is in line with yours.

Thank you, we will add this reference to reinforce our result.

Minor comments

Please replace ‘Hydrological’ with ‘Hydrographic’ throughout.

Ok, totally agree.

Figure 1 is busy and therefore making an effort to explain all the signs is important. For example, you should indicate what the stars represent early on. You may also want to add the names of the different NAC branches here.

Yes, we agree Figure 1 is busy and with a lot of information necessary to understand the paper. The meaning of the stars is already indicated in the Figure caption of Fig. 1. We will add NNAC, SAF, SNAC and IC (Irminger C.) in the figure.

lines 251: Please keep it consistent with the decimal throughout the paper.

Ok, thank you, we will add one decimal to be consistent throughout the paper.

The bathymetry can hardly be seen in the AVISO figures.

Right, we will draw the bathymetry with thicker gray lines.

lines 505: Define the SPG acronym. And no need for the SPG acronym in the last paragraph of the discussion.

Right, in any case that part of the discussion will be rewritten, and the definition of the SPG will be done in the introduction.

Caption Fig. 9; It is not clear in the text that the anomalies are for 2014.

The referee is right, we will explicitly indicate that it is the 2014 anomaly.

Anonymous Referee #2

Received and published: 16 August 2017

The GEOVIDE cruise in May–June 2014 reveals an intense Meridional Overturning Circulation over a cold and fresh subpolar North Atlantic, by Patricia Zunino et al. This paper discusses the physical background of the GEOVIDE cruise in 2014. It highlights changes in transport as well as heat and freshwater content compared to the 2002–2012 mean state. The most interesting conclusion is that the large scale cooling seen in the SPG is (more then) compensated by a strengthened circulation in the net heat transport.

One comment on the structure of the paper. Although the TEI measurements do not feature in the abstract there are discussed several times in the introduction and elsewhere in the paper. It therefore reads like the discussion of the TEI measurements will be discussed later in the paper, but this never happens. It is also never mentioned where (in which other paper) these measurements will be shown. This does not improve the overall clarity of the paper. The authors should rephrase the text as to make it more clear what the focus of this paper is, why it is presented in Biogeosciences and where the other data from the GEOVIDE cruise is (or will be) presented.

We understand that it can be somehow uncommon to publish a physical paper in Biogeoscience. However, our paper is part of a special issue in Biogeosciences with all the papers resulting from the GEOVIDE cruise. This is why our paper, which defines the physical background of the GEOVIDE cruise, has been submitted to Biogeoscience. In order to make it clearer, we will introduce some references at the end of the introduction and at the beginning of the section 3.4 in the new version of the manuscript.

The discussion section can be improved. Where increases and decreases are discussed (for example the second paragraph) the authors should mention whether this increase is statistically significant or fall with the observed variability.

Ok, we think that we did not introduce enough the ideas in each paragraph, so we will always begin the paragraph with a description of the transport anomaly, including its significance. Actually, we only discussed the NAC and Irminger C. that showed a significant variability in their different components, although their overall transport did not. Paragraph 2 of the discussion (line 392) could begin by:

“When defining the IC as in D2016, we saw an increase in the IC intensity in 2014, but within the observed variability (Table 1). However, the such-defined IC encompasses a warm and salty northward transport and a cold and fresh southward transport. So, to go further [...]”

At the beginning of paragraph 3 (line 402), we propose: “Concerning the weaker NAC, its 2014 intensity, 32.2 ± 11.4 Sv, is weaker although in the limits of the observed variability (41.8 ± 3.7 Sv). By the decomposition of this wide current, it is very likely [...]”

In the discussion on the origin of the cooling of the SPG, advection versus surface fluxes, it is important to consider the time scale that both are acting on. The changes in advection are thought to act on longer (decadal) time scales while the surface forcing has a more direct effect. In fact, the warming trend in the western SPG was halted much earlier than 2014 and much has been explained by surface forcing (Piron, 2015; de Jong and de Steur, 2016;

Yashayaev and Loder, 2017). I would encourage the authors to put the 2014 anomalies into context of the recent interannual variability rather than focusing on a comparison with the mean.

This is the general critique done by the three reviewers. We agree that the changes in the lateral advection affect the heat and freshwater content changes at decadal timescale. We also agree that the air-sea flux is thought to cause heat and freshwater changes in the ocean at shorter period of time, buffering or intensifying the effect of the lateral advection. A more detailed answer is given in the introduction of this document. We will reorganize and expand the third paragraph of the introduction and the discussion of the ms in order to be clearer in the timescales of both processes creating thermohaline anomalies in the SPNA (see also answers to reviewer #1 comments).

Comments

- Suggest to replace MOC with AMOC (Atlantic MOC) throughout the paper since it is more appropriate in the context of the North Atlantic circulation discussed here.

We agree that the MOC is a general term for the Meridional Overturning Circulation affecting all the oceans. So we will use “AMOC” in the introduction, but keep “MOC” in the result for consistency with other references (Mercier et al. 2015 and Daniault et al. 2016). Actually, we should even call it OVIDE MOC in the results but we prefer to keep it simple.

- Line 63: “the ocean has taken up 90% of the heat accumulated”.

Right, we will modify it.

- Line 74: not sure what is meant by durable.

It means persistent in time. In any case that sentence will be removed of the ms since the third paragraph of the Introduction will be re-structured.

- Lines 139-141: this criterion seems to lead to unexpected values near the shelf of Greenland. The waters in the IC and EGC are very stratified, but the orange line shows WMLD as deep as in the central Irminger Sea.

It was a mistake, there should have been no value here, Actually, the WMLD cannot be determined west of station 48 because of the strong layering in the East Greenland/Irminger Current.

- Line 221: This current system is not commonly known as the WBC. Elsewhere the authors refer to the East Greenland (Coastal) Current and the Irminger Current which is more appropriate.

The “western boundary current” is used in many papers referring to the currents over whole water column in the western side of the oceans (see for exemple “Moored Observations of Western Boundary Current Variability and Thermohaline Circulation at 26.5° in the Subtropical North Atlantic” of Lee et al. (1996) or “The western boundary current of the seasonal subtropical gyre in the Bay of Bengal” of Shetye et al. (1993). In our region, we have referred to this dynamic structure as WBC following Daniault et al. (2016). The Western

Boundary Current was defined as the sum of the East Greenland Irminger Current and the Deep Western Boundary Current. The former is composed by three components: the East Greenland Current, the spill jet and the adjacent IC that usually cannot be separated at 60°N. In our paper we were referring to the water flowing southward at the western side of the Irminger Sea, west and below the Irminger Gyre. Furthermore, when we talked about the Irminger Current, we were specifically referring to the water flowing northeastward west of the Reykjanes Ridge, although it is true that it recirculates in the East Greenland/Irminger Current (Pickart et al., 2005). In any case, we will rewrite this part of the manuscript to be clearer, but we consider that WBC is the appropriate term here.

- Line 252: “Note that the net transport in the northern branch is null”.

Thank you, we will simplify this sentence.

- Line 274: “as well as it can“ is not very readable. Even though I understand that the author is not a native English speaker I think the readability would improve if the authors took another critical look at the grammar of some of the sentences in this manuscript.

Ok, we will change “as well as it can ...” by “and they can ...”. Yes, we are not English speaker, this is why our ms was already revised by a professional native English speaker.

- Line 297: the section just seems to miss (cut south off) the high energy signal of the Irminger Current on the RR.

We do not understand what the referee refers to. In this paragraph, we are discussing about the large eddy near Eriador Seamount. The Irminger Current is quite far away to the northwest.

- Regarding the paragraphs between lines 284 and 325. The red squares in Figure 6 are mention, but the others are not. It would be easier to follow the eddy description if the yellow, green and orange squares were also denoted here.

Totally right. Actually, the colored squares were introduced in the figure to make easier the eddy identifications. In the new version of the manuscript we will better indicate all of them.

- Lines 359-361: not clear which anomalies are referred to here. If it is the cooling/freshening in the western SPG (caused by ventilation) it is not surprising to see it linked to an oxygen increase.

Maybe the term “zooming out” was misunderstood. When we talked about ventilation, we were indeed referring to the oxygen positive anomaly, so we will precise Figure 7c. This paragraph was written to give a general view of the link between temperature, salinity and oxygen anomalies. So we will slightly modify this sentence to make it clearer.

- Lines 371-380: Please let the reader know where the data from these other measurements will be presented if not here.

We will include references to the other papers of the Geovide special issue in Biogeoscience in the introduction and in section 3.4.

- Line 430: Briefly mention why is 1997 excluded.

We modified the sentence as “To compare it with the 2002-2010 average, we used the data of Mercier et al. (2015), without data from 1997 because it did not belong to our reference period, [...]”.

- In the discussion on freshwater surface fluxes it would be good to mention something about the uncertainties of these fields over the ocean.

Right, we already thought about this complex issue, because uncertainties in evaporation and precipitation products are very difficult to assess (Dee et al., 2011). So Josey and Marsh (2005) made an estimate by comparing NCEP and ERA-40 products. We did the same in our case. The difference between monthly freshwater fluxes over the region 40°N-60°N, 45°W-10°W estimated with NCEP and ERA-INTERIM is about 10 % of the absolute values. Over 2002-2015, no clear bias stands out between both products and accumulating fresh water fluxes over years does not increase the relative difference of 10 %. The accumulated air-sea freshwater flux of $2 \times 10^{12} \text{ m}^3$ from 2013 to 2014 that was shown in Figure 10 (ERA-IN) is different by $4 \times 10^{11} \text{ m}^3$ from the NCEP estimate; we will discuss about these errors for the period 2013 to 2014 in the new version of the ms and add the NCEP estimate in Figure 10, which will be Figure 12 in the new version of the ms.

Anonymous Referee #3

Received and published: 21 August 2017

In this manuscript the authors present the results from analysis of a 2014 CTD section taken along the OVIDE section. The cruise was a contribution to the GEOTRACES program and so the results of this hydrographic analysis will allow analysis of the extensive chemistry data also collected on the cruise. The authors describe the OVIDE section from the cruise data, place it in context of data along the OVIDE section from 2002 to 2012, and attempt to explain some of the differences.

The paper is a good, straightforward description of a cruise data set, and gives a highly valuable look at the MOC and gyre circulation of the eastern subpolar North Atlantic in summer 2014. The text is well written and the figures are relevant and mainly well presented. The weakness of the paper lies in the authors attempt to understand the reasons for the cooling and freshening they observe in the 2014 section eastern basins compared to the earlier data. The introduction is a little muddled on this topic, and the conclusions that they draw from their analysis are not as robust as they could be. Below are some comments that I hope the authors can use to improve that aspect of the paper, as well as some minor edits.

1. Timescales of change. The authors have missed a key aspect of the literature on changes in the subpolar North Atlantic, and that is about timescales. If you could rewrite the introduction considering the timescales of each of the papers that you cite it would help you focus your own analysis. In short, the arguments for ocean heat transport convergence being the primary control are all on long timescales – multiyear at least, certainly decadal. The "cold blob" analyses and the evidence for air-sea fluxes are all about short timescales - seasonal to a year or two. You should also consider the possibility that temperature anomalies and salinity anomalies may have some different forcing mechanisms on different timescales. You may not have enough data to look at long-term changes, and a focus on the short term may be more appropriate with the analysis that you have done already.

Yes, as indicated in the introduction of this document, we agree that the mechanisms controlling the heat and freshwater content changes in the ocean at different time-scales were not well exposed in the manuscript. We will reorganize the last part of the introduction and the last part of the discussion to account for this. We will put the “inter-annual” signal of 2013-2014, which is an intensification of the cooling already started in mid-2000s as documented by Robson et al. (2016;2017), and shown in this manuscript to be dominantly caused by the air-sea flux.

2. Methods. I realize that the authors are using well-developed methods described in earlier papers from the group, but a little bit more information would help the reader understand their method. In particular I was not sure whether the SADCPC data are used in the inversion. I had thought they were, so it is surely not a surprise that the main features in the SADCPC data are also seen in the solution?

Yes, as it is indicated in the manuscript in line 144 – 145, the SADCPC data are used to constrain the inverse model. To make it clearer, just after the first sentence, we will add the sentence “For inversion constrain, the S-ADCP data were averaged between stations in layers where the shear of the velocity profile was consistent with geostrophic velocity profiles”. The referee is right: it is not a surprise that the main features in the SADCPC data are also visible in the inversion solution. However, we wanted to show how the small-scale features visible in the SADCPC data were averaged in the inversion because of the coarser resolution of the hydrographic profiles (lines 161-163).

I felt there should be more information about the reduced resolution of the CTD spacing in 2014. You say in lines 123-124 that you will later show that the features were "correctly sampled", but your evidence for this in lines 386-387 seems to be just that all the circulation features are identified (Table 1). I would like to see this explored more – is the higher uncertainty in Table 1 because of the resolution? If you subsample an earlier cruise at the 2014 resolution do you get the same results as the original resolution?

There are several points in your questions.

First, we did sensitivity study on the 2010 data to determine the optimized sampling for the GEOVIDE cruise. The 2010 transport data showed the same results with the original high resolution and the GEOVIDE resolution, but indeed, errors on regional features increased when subsampled. However, in 2014, we used an OS38 (the latest generation of SADCP with a 1200m range), and could average the constrains in a deeper layer (more geostrophic) with less uncertainties than all the previous surveys where a NB75 was used. This is why, at the end, the errors in transports are quite similar in GEOVIDE and in the previous OVIDE surveys. This information will be synthesized in section 2.2 in the new version of the manuscript.

Second, in table 1, the 2014 errors were calculated from the covariance matrix resulting from the box inverse model, while the errors given for the means (2002 - 2012) were standard deviations of the six estimates of the different currents. In fact, because the transport estimates of the currents are more or less stable during the 2002 – 2012 period, their standard deviations are low compared to the error given for each single OVIDE cruise. The information about how the errors were computed will be introduced in the table caption in the new version of the manuscript.

It would be useful to have more explanation about how you computed the gyre and overturning heat transport (lines 267-270)

We will add "(their equation (1))" line 269 after referring to Mercier et al. (2015). We prefer not to expand this topic because it is not a new result: one of the most important results of Mercier et al. was indeed that the MOC was the primary driver of the heat flux across the OVIDE section. We just wanted to complement their time series.

3. I struggled to see the importance or relevance of section 3.2 (fronts and eddies). This looks like a description that will be useful for colleagues who are writing papers on the GEOTRACES data, but it seems to sit a little uneasily in the context of the rest of the paper. The same can be said for section 3.4. I can imagine that these lines of text could be usefully transferred into a companion paper.

Yes, we agree that 3.2 and 3.4 sections are not so relevant as results. Nevertheless, one of the objectives of this paper was to define the physical background of the GEOVIDE cruise, which is very important for the interpretation of the TEIs distribution to be carried out by our GEOTRACES colleagues. In fact, this paper has been submitted to Biogeoscience Discussion as part of the GEOVIDE Special Issue, where all the GEOVIDE papers are going to be submitted. So, we consider that we can leave both sections in our physical paper, inside this Biogeoscience Special Issue. Nevertheless, we will introduce more information about the other GEOVIDE papers in section 3.4 in the new version of the manuscript.

4. Thermohaline anomalies. You need to state how you computed the anomalies - presumably on pressure surfaces.

It was indicated how the anomalies were estimated at the beginning of the first paragraph of section 3.3 as: “In the following, S and T anomalies were quantified as the mean values of the anomaly patches represented in Fig. 7.” Following the remark of the reviewer, we will add in this paragraph that those anomalies were computed in pressure coordinates. Density coordinates are generally more appropriate, but it makes the interpretation much trickier and does not substantially change the conclusions of our study.

Your description would be more easily followed if you related the anomaly patches to the circulation features that you have already described. For example, is the first anomaly (lines 333-334) in the Irminger Current?

Good idea. So we will transform the sentence as: “First, negative anomalies in surface-intermediate waters were observed above the WMLD over the Reykjanes Ridge (in the IC and the ERRC) and east of 20° W (in the SNAC and its recirculation)”.

The deeper anomalies are associated with the variability of waters masses (LSW and ISOW) and not specifically to dynamical features. The anomalies in the Mediterranean Water were already associated with eddies.

If the anomalies are focussed in the main currents (IC, NAC) could that be evidence for ocean transport as a source of the anomalies?

Lines 355-358 suggest that the displacement of the SAF (i.e. central NAC) is preponderant in the fresh and cold anomalies at 23°W. However, we did not really interpret the anomalies in the ERRC and IC with the lateral advection, although, as you suggest, it is surely an advected signal. See below for a more precise answer.

An important point: I do not agree that the bottom of the anomalies is at the depth of the winter mixed layer - in most cases they extend deeper than the WMLD, which is surely significant and counter evidence for your hypothesis of air-sea fluxes being the key driver.

We agree, we did not put enough weight on the advective origin of some anomalies, and precisely the anomaly in the ERRC. Thank you for this interesting remark. So, to answer your remark and improve the manuscript, we will reformulate lines 333-336 by:

“First, negative anomalies in surface-intermediate waters were observed above the WMLD over the Reykjanes Ridge (in the IC and the ERRC) and east of 20° W (in the SNAC and its recirculation). In the former, the S and θ anomalies were quantified at -0.08 and -1.04 °C, respectively. In the latter, the negative anomalies of S and θ amounted to -0.11 and -0.70° C. In the ERRC, negative S and θ anomalies also appeared below the WMLD amounting to -0.06 and -0.80 °C, respectively. It concerns a water mass that is different from the one in the WMLD; both water masses are separated by a negative anomaly of oxygen (Fig. 2c) and a maximum of potential vorticity (not shown).”

Then, in the discussion, we will also reformulate lines 484-487 as:

“More evidence for the important role of air-sea fluxes is provided by the distribution of θ , S and oxygen anomalies in the water column. Indeed, the WMLD along the OVIDE section east of 20° W coincided with the deep limit of the anomalies (Fig. 7). It is somewhat more complex in the ERRC, where the WMLD crosses the anomaly separating subpolar mode water (SPMW) and upper Labrador Sea Water (LSW), see Fig. 2b; both water masses were advected together by the ERRC, but probably issued from different ventilation regions. According to de Boisséson et al. (2012), the SPMW is formed by air-sea interactions on its way around the Iceland basin.”

line 360 and elsewhere - it is best to avoid subjective words like "remarkably" especially when you do not explain what is remarkable about that observation.

Ok, we checked the whole ms and we can and we will remove this adverb everywhere, and reformulate when necessary.

5. Discussion. This section needs some improvements because the writing becomes less clear and sometimes less focussed. Paragraph 2 (lines 392 onwards) is very unclear. I'm not always sure which data set or feature you are referring to when you quantify the transport, and how that relates to Table 1. You conclude that the Irminger Current is significantly strengthened in 2014, but from the numbers in Table 1 it looks as they are not significantly different within the error bars (the uncertainty on the 2014 estimates are large).

We will make the following changes to improve the clarity of the message. First, we will introduce the paragraph 2 by:

“When defining the IC as in D2016, we saw an increase in the IC intensity in 2014, but within the observed variability (table 1). However, the such-defined IC encompasses a warm and salty northward transport and a cold and fresh southward transport. So, to go further [...]”.

We will also add a specific column in Table 1 for the transport of the part of the IC that flows northward, which is the one that differs significantly from the mean of D2016.

para 4 (line 413 onwards). It is interesting to me that the SAF has shifted southeastward (by how much?).

It is indicated in the manuscript, approximately 100 km along the OVIDE section (line 414), and this is consistent with the SAF displacement observed in the ADT (see Figures 3 in this document and comments in the answer to Reviewer 1). To make it clearer, we will add to the ms the ADT figure (Figure 3 in this document) and discuss it in the fourth paragraph of the Discussion section.

Does this actually imply that the Bersch mechanism for freshening of the eastern basin might be at work, even though you are arguing for this not being the source of the freshening?

At the end of the discussion of the manuscript we briefly discussed about the Bersch mechanism. Inspired by your remark, we pushed further and answer no, our observations lead us to conclude that the freshening at short timescales is not associated with more advection of subpolar water into the eastern SPNA. So we will remove the last paragraph of the discussion (lines 520-527) that was related to the observations of Bersch et al., but add this information to the fourth paragraph of the discussion about the southeastward displacement of the SAF (line 413-418), as follows:

“The SAF, that bears the central branch of the NAC, shows also a remarkable southeastward displacement in 2014 in relation to the mean circulation pattern (station 26 in Fig. 1), of about 100 km. A careful study of the ADT streamlines (Fig. 8) showed that this displacement was not due to a peculiar meandering of the front and that the SAF was actually narrower and located more to the southeast in 2014, when compared to the 2002–2012 mean. Bersch et al. (2007) linked the northwestward displacement of the SAF in the eastern North Atlantic in the late 1990's to a shift from positive to negative values in the index of the North Atlantic Oscillation (NAO), which is the dominant mode of atmospheric variability over the North

Atlantic. After a decade of neutral values, the winter NAO index turned positive in 2011 and continued positive in 2013 and 2014 (Hurrell et al., 2017). The southeastward displacement of the SAF is thus symmetric to Bersch et al. (2007) and consistent with their observations.”

You need to explain why the Marsh and Grist papers are relevant to this work, since they refer to a different branch of the NAC that does not come here - what is the connection?

Yes, the referee is right, they referred to a different branch of the NAC. The connection here is just to compare our result about the southeastward displacement of the SAF with other works, but obviously, it blurs the picture since it is further south, so we will delete these 2 sentences about Grist et al...

Finally, I come back to my point about timescales of forcing. I think your result that the heat transport is high even though the upper ocean is cooler is interesting, but I don't agree that it is necessarily contrasting with the results of Desbruyères et al. The air-sea fluxes that you present are a great result - but they are only for 1 year, and many of the papers that you refer to are talking about ocean transport convergence as the primary factor over longer timescales.

Yes, we agree with the referee, the explanation of the changes at different time scales and the mechanisms generating them is the first point to improve in this manuscript. In relation to the Desbruyères et al., we want to keep the contrast with Desbruyères et al. (2015), making it clearer, so we propose in line 449-453 this sentence instead:

“This result might be the effect of a short-term variability since it contrasts with the study of Desbruyères et al. (2015), who argued that the long-term variability of the ocean heat transport at the OVIDE section is dominated by the advection by the mean velocity field of temperature anomalies formed upstream rather than the velocity anomalies acting on temperature”.

It is not correct to say that the 2014 anomaly comes after 18 years of warming and salinification - papers by Robson, Holliday, and the ICES Report on Ocean Climate show observed declining temperatures and salinity in these eastern basins since the late 2000s, part of multi-year variability.

Yes, totally right, the sentence “*The 2014 anomaly was the first detected, after approximately 18 years of warming and salinification*” is going to be deleted in the new version of the manuscript because it is wrong.

That said, the obs also show a sharp drop in salinity and temperature in recent years, so it seems likely that the longer term changes in circulation are being reinforced by enhance air-sea fluxes. It might help if you focused the discussion on a short term atmospheric influence, superimposed on a longer term trend.

Exactly, as it has been previously exposed in this document, this is what we are going to do in the new version of the manuscript. We will even add “at short-time scale” in the last sentence of the abstract: “We concluded that, at short-time scale, these changes were mainly driven by air-sea heat and freshwater fluxes rather than by ocean circulation”.

Minor edits

- Lines 88-89, Holliday et al does not look at the Irminger Sea. Their hypothesis was about a shift of the subpolar front (the Bersch mechanism) not advection.

Right only Iceland basin, we will remove Irminger in this line.

About their hypothesis, actually, we were referring to the sentence “The decrease in potential temperature and salinity after 2010 in all basins provides the first new evidence that the eastern subpolar Atlantic is once again influenced by cold, fresh western subpolar water.” (paragraph 5, section 5 of Holliday et al. (2015)”. So we will explicitly quote Holliday et al. to clarify.

- line 144 (and elsewhere) "hydrological" should be replaced with "hydrographic"

Yes, we will change it everywhere.

- line 219 use "Fig. 3b" rather than "Fig. 3, lower panel"

Yes, right.

- line 239 what do you mean by barotropic streamfunction here? You are referring I think to the plot of accumulated transport - is that the same thing?

Yes, the barotropic streamfunction is the volume transport vertically accumulated and horizontally accumulated from Greenland to each station. We will indicate it in the new version of the manuscript.

- line 246 and Fig. 5, I find the green dots hard to see - can you use a color that stands out more clearly?

Yes, we will change it to white dots.

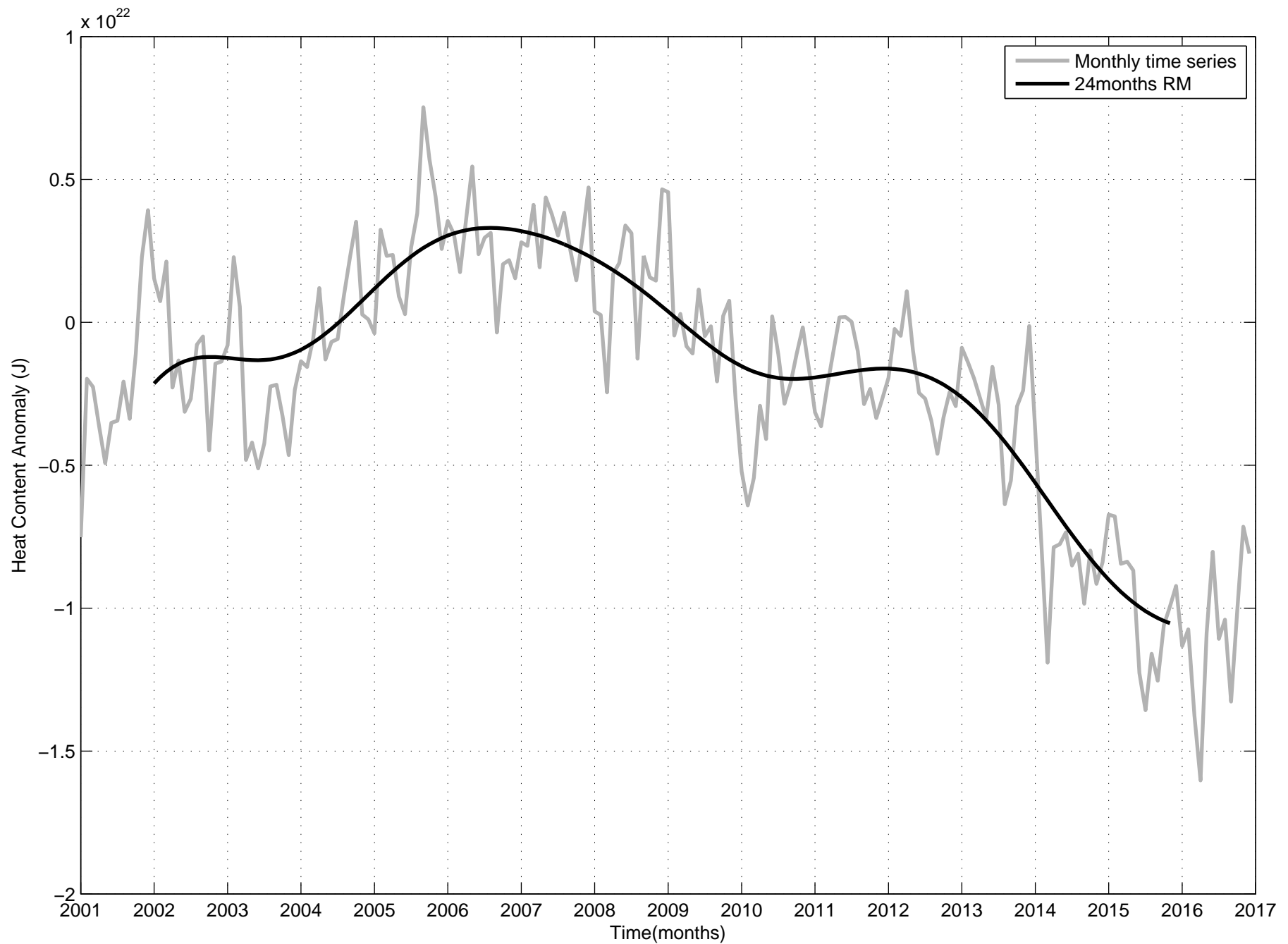


Figure 1: Heat content anomalies in relation to the mean heat content for the period 2002 - 2012 in the upper 1000m of the region 40°N-60°N and 45°W-10°W. Grey line is the monthly time series; black line is the 2-year running mean of the monthly time series. Data source: EN4 database (Good et al. 2013).

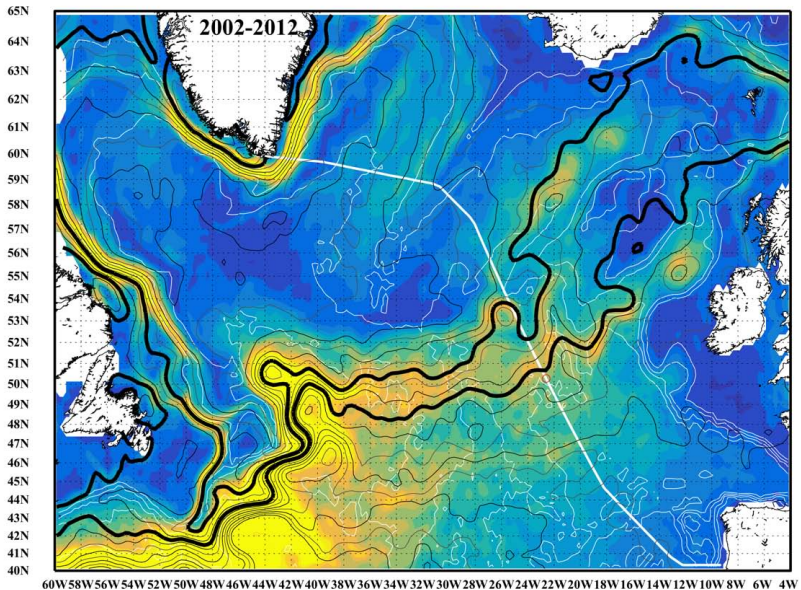
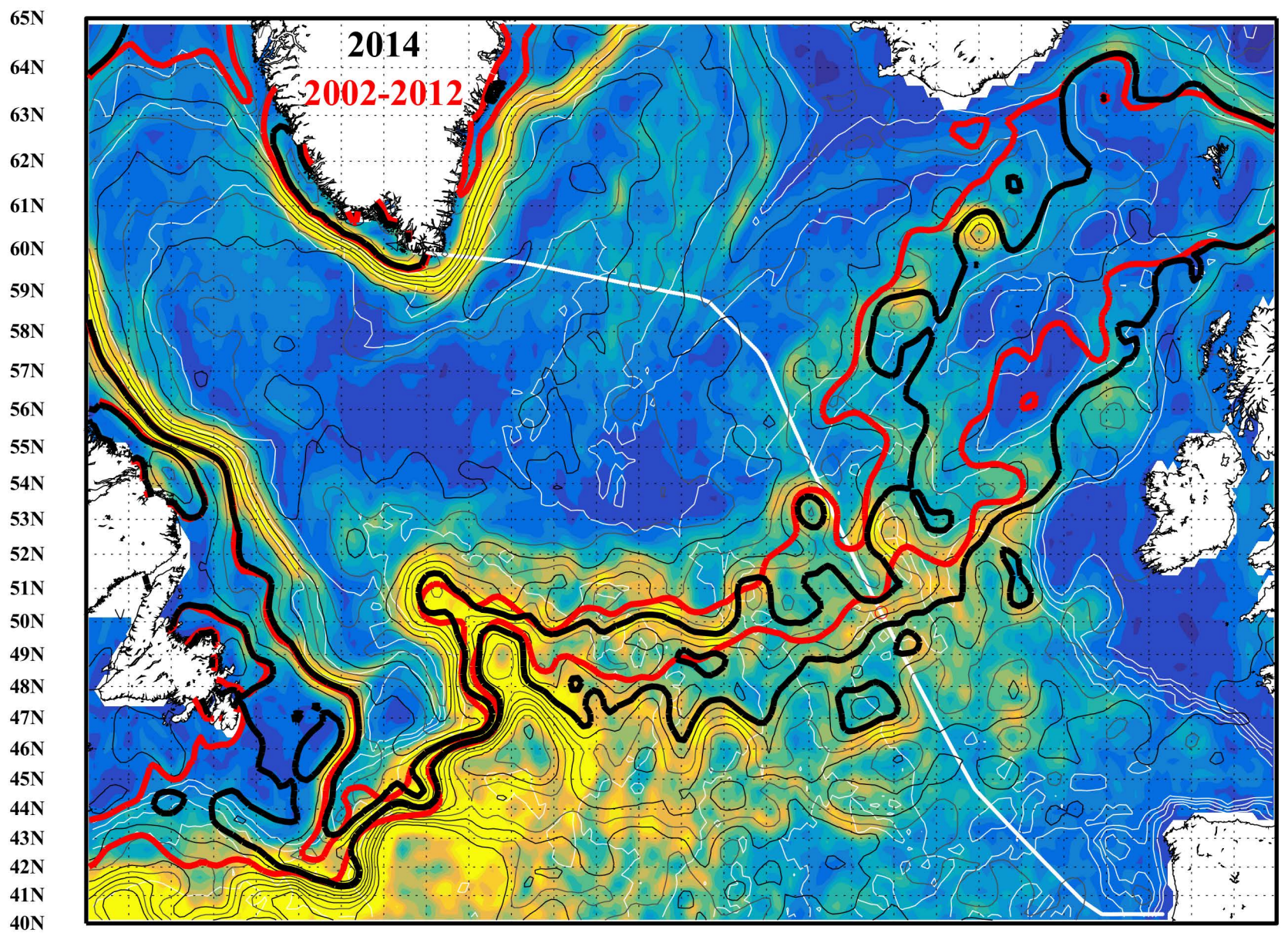


Fig. 2: Contours of the Absolute Dynamical Topography averaged over 2002-2012 (in black and grey), after removing the overall trend of 2.8mm/yr. Contours are every 0.05m. Thick contours correspond to the levels encompassing the SAF front during OVIDE cruises.



60W 58W 56W 54W 52W 50W 48W 46W 44W 42W 40W 38W 36W 34W 32W 30W 28W 26W 24W 22W 20W 18W 16W 14W 12W 10W 8W 6W 4W

Figure 3: Contours of the Absolute Dynamical Topography averaged over 2014 (in thin lines). Contours are every 0.05m. Thick contours correspond to the levels encompassing the SAF front during OVIDE cruises: bold red lines for the mean 2002 – 2012 and bold black lines for 2014. Note that the temporal trend on the mean ADT over the whole box (2.8mm/yr) was removed. Bathymetry (1000m step contours) and the OVIDE section are plotted in white. Colors represent the absolute velocity of the current (yellow for velocities stronger than 0.3m/s). This figure will be added to the new ms.

1 **The GEOVIDE cruise in May-June 2014 reveals an intense Meridional**
2 **Overturning Circulation over a cold and fresh subpolar North Atlantic**

3

4 Patricia Zunino¹, Pascale Lherminier², Herlé Mercier¹, Nathalie Danialt³, Maribel I. García-
5 Ibáñez⁴ and Fiz F. Pérez⁴

6 ¹ CNRS, Laboratoire d'Océanographie Physique et Spatiale (LOPS), IUEM, Plouzané, France.

7 ² Ifremer, Laboratoire d'Océanographie Physique et Spatiale (LOPS), IUEM, Plouzané, France.

8 ³ Université de Bretagne Occidentale, Laboratoire d'Océanographie Physique et Spatiale (LOPS),
9 IUEM, Plouzané, France.

10 ⁴ Instituto de Investigaciones Marinas, IIM-CSIC, 36208 Vigo, Spain

11 Corresponding author: pzuninor@ifremer.fr

12

13 **Abstract**

14 The GEOVIDE cruise was carried out in the subpolar North Atlantic (SPNA), along the
15 OVIDE section and across the Labrador Sea, in May-June 2014. It was planned to clarify the
16 distribution of the trace elements and their isotopes in the SPNA as part of the GEOTRACES
17 international program. This paper focuses on the state of the circulation and distribution of
18 thermohaline properties during the cruise. In terms of circulation, the comparison with the
19 2002–2012 mean state shows a more intense Irminger current and also a weaker North
20 Atlantic Current, with a transfer of volume transport from its northern to its central branch.
21 However, those anomalies are compatible with the variability already observed along the
22 OVIDE section in the 2000s. In terms of properties, the surface waters of the eastern SPNA
23 were much colder and fresher than the averages over 2002–2012. Remarkably, in spite of
24 negative temperature anomalies in the surface waters, the heat transport across the OVIDE
25 section, estimated at 0.56 ± 0.06 PW, was the largest measured since 2002. This relatively
26 large value is related to the relatively strong Meridional Overturning Circulation measured
27 across the OVIDE section during GEOVIDE (18.7 ± 3.0 Sv). Analyzing the air-sea heat and
28 freshwater fluxes over the eastern SPNA in relation to the heat and freshwater content
29 changes observed during 2013 and 2014, we concluded that, **at short time-scale**, these

30 changes were mainly driven by air-sea heat and freshwater fluxes rather than by ocean
31 circulation.

32 **1. Introduction**

33 The subpolar North Atlantic (SPNA) is a key area for studying the effect of climate change in
34 the ocean. The deep convection processes there behave as a driving mechanism for the
35 Meridional Overturning Circulation (Kuhlbrodt et al., 2007; Rhein et al., 2011; Sarafanov et
36 al., 2012), which transports heat to high latitudes in the North Atlantic and is predicted to
37 slow down at the end of the present century (IPCC, 2007). Additionally, the SPNA presents
38 the highest anthropogenic CO₂ storage rate of all oceans (Khatiwala et al., 2013), due to both
39 the advection of surface waters enriched with anthropogenic CO₂ in the subtropical North
40 Atlantic (Pérez et al., 2013; Zunino et al., 2015) and their deep injection in the subpolar gyre
41 (Pérez et al., 2010). In addition, the SPNA is one of the few oceanic regions where significant
42 cooling was detected over 1955–2010 while the rest of the world oceans was warming
43 (Levitus et al., 2012). For all these reasons, the SPNA has been the target of several projects
44 and broadly sampled by oceanographic cruises. As part of the OVIDE project
45 (<http://www.umr-lops.fr/Projets/Projets-actifs/OVIDE>), the OVIDE section has been sampled
46 biennially in summer since 2002 to collect data related to the circulation and the carbon cycle.
47 Its path between Greenland and Portugal is shown in Fig. 1 along with a schematic view of
48 the upper, intermediate and deep circulations in the SPNA adapted from Danialt et al.
49 (2016), which will be referred to as D2016 hereafter.

50 The international GEOTRACES program (<http://www.geotraces.org/>) aims to characterize the
51 trace elements and their isotopes (TEIs) in the world ocean. These TEIs are Fe, Al, Zn, Mn,
52 Cd, Cu, $\delta^{15}\text{N}$, $\delta^{13}\text{C}$, $^{231}\text{Pa}/^{230}\text{Th}$, Pb and Nd in the dissolved phase as well as in particles and
53 aerosols. TEIs provide constraints and flux estimates that can be used to reconstruct the past
54 environmental conditions. The GEOVIDE project is a French contribution to the
55 GEOTRACES program. It is dedicated to measure the large-scale distributions of TEIs in the
56 SPNA for the first time. The GEOVIDE cruise was carried out in May–June 2014 and was
57 composed of two sections: one along the OVIDE line (its 7th repetition) and another one
58 crossing the Labrador Sea, from Cape Farewell (Greenland) to St John's (Canada). The
59 expertise gained on water mass properties and circulation across the OVIDE section (García-
60 Ibáñez et al., 2015; D2016) first helped to determine the optimal geographic distribution of
61 the TEI sampling. However, the ocean is not steady, and the present study shows how
62 anomalous, in terms of thermohaline properties and circulation, the eastern SPNA was in

63 summer 2014 compared with the previous decade, and thus provides guidance for the
64 interpretation of the measured distribution of TEIs.

65 The ocean has ~~uptaken~~ **uptaken up** 90% of the heat ~~energy~~ accumulated in the climate system since
66 1971 (Riser et al., 2016). In this context, it is striking to note the absence of a significant
67 warming trend in between 50° N and 60° N in the Atlantic Ocean **between 1955 and 2010**
68 (Levitus et al., 2012; Sgubin et al., 2017). **In fact, an important variability in the heat and**
69 **freshwater content occurs in the SPNA at the decadal or longer time-scales. Since 1960,**
70 **different periods of cooling (warming) or freshening (salinification) in the SPNA have**
71 **been detected. Negative salinity anomalies were observed in the SPNA surface waters**
72 **during the 1970s, and referred to as the Great Salinity Anomaly event. They were**
73 **explained by a large pulse of freshwater getting into the SPNA through the Denmark**
74 **Strait (Dickson et al. 1988; Robson et al., 2014). Concurrently, the subpolar gyre (SPG)**
75 **started a cold phase that persisted up to the beginning of the 1990s. Later, from mid-**
76 **1990s to mid-2000s, positive anomalies of temperature and salinity in the surface waters**
77 **of the SPNA were observed, coinciding with the contraction and weakening of the SPG**
78 **(e.g. Bersch, 2002; 2007; Sarafanov et al., 2008; Häkkinen et al., 2011). However,**~~a strong~~
79 ~~variability occurs at the decadal timescale, with, in particular, warming and salinification of~~
80 ~~the SPNA detected from the mid-1990s to the mid-2000s (Bersch et al., 2007; Sarafanov et~~
81 ~~al., 2008).~~ **Many works analyzed the causes of the observed decadal to multi-decadal**
82 **variability in ocean heat content in the SPNA by analysis of both observations and**
83 **model outputs (e.g. Some studies identified the North Atlantic Oscillation (NAO, Hurrell et**
84 ~~al., 1995) as a key atmospheric forcing explaining this variability. The reduction in the~~
85 ~~buoyancy forced deep convection in the Labrador Sea was associated with the decline in the~~
86 ~~NAO index after 1996 and was identified as the cause of the observed warming, salinification~~
87 ~~and concurrent contraction/weakening of the subpolar gyre (Bersch, 2002; Häkkinen and~~
88 ~~Rhines, 2004; and Bersch et al., 2007). Robson et al. (2012) found that the rapid warming of~~
89 ~~the SPNA was primarily caused by durable northward ocean heat transport associated with the~~
90 ~~strengthening of the Meridional Overturning Circulation (MOC) in response to the increased~~
91 ~~surface buoyancy loss in the Labrador Sea during the prolonged positive NAO period in the~~
92 ~~late 1980s to early 1990s (see also Deshayes and Frankignoul, 2008; Lohmann et al., 2009;~~
93 **Robson et al., 2012; 2014; and**Barrier et al., 2015). **They concluded that the heat content**
94 **anomalies in the SPNA at long time-scale are mainly controlled by changes in the lateral**
95 **advection, linked to changes in the intensity of the Atlantic Meridional Overturning**

96 **Circulation (AMOC). At shorter period of time, the air-sea flux causes significant heat**
97 **and freshwater changes, by intensifying or buffering the effect of the anomalies caused**
98 **by the lateral advection (Barrier et al., 2015; Desbruyères et al., 2015; Grist et al., 2015).**

99 ~~Other studies identified anomalies in the wind forcing in the inter-gyre-gyre region as the~~
100 ~~cause of the 1995-1996 warming and salinification (Herbaut and Houssais, 2009; and~~
101 ~~Häkkinen et al., 2011).~~

102 Recently, **Hermanson et al. (2014) and Robson et al. (2016; 2017), analyzed outputs of**
103 **coupled climate models, and identified a new cooling and freshening period from the**
104 **mid-2000s. Their results coincide with observations:** Johnson et al. (2016) documented a
105 SPNA region cooler in 2014 than in 1993-2014 climatology, this cooling intensified in 2015
106 and 2016 (Yashayaev and Loder, 2016; 2017). ~~So, the GEOVIDE cruise crossed the SPNA~~
107 ~~region in a context that contrasts with the previous decade and could be the beginning of a~~
108 ~~new state.~~ Over the eastern SPNA, Grist et al. (2015) analyzed the winter 2014 anomalous air-
109 sea fluxes and their imprint on the ocean. Based on EN4 ocean reanalysis, they detected
110 negative temperature anomalies in the surface waters, which they related to anomalous air-sea
111 heat fluxes. Conversely, Holliday et al. (2015), who found evidence of similar cooling and
112 also of freshening in the ~~Irvinger~~ and Iceland basins from 2010–2011 to 2014, privileged the
113 hypothesis of a remote source of those anomalies, **writing that** i.e. “**the eastern SPNA is once**
114 **again being influenced by cold, fresh advection from the western subpolar water**”~~SPNA.~~
115 We will discuss both hypotheses in this study.

116 In this article, we first contextualize the physical background of the GEOVIDE cruise to help
117 for the interpretation of distribution of TEIs in the eastern SPNA. **The works dealing with**
118 **TEIs distribution will be published in this Biogeoscience GEOVIDE special issue: Cossa**
119 **et al. (2017), Lemaître et al. (2017), García-Ibáñez et al., (2017), and other manuscripts**
120 **are in preparation.** Subsequently, by the analysis of the GEOVIDE cruise data along with
121 altimetry, oceanic database and air-sea flux data, we disentangle the causes of the anomalous
122 thermohaline properties of the surface and intermediate layers of the eastern SPNA in May–
123 June 2014. The paper is organized as follows. Data and methodology are described in section
124 2. Section 3 displays the main results on the large and mesoscale patterns of the circulation
125 and thermohaline anomalies in 2014, settling the GEOVIDE TEIs stations in this context.
126 These results are discussed in section 4. Finally, section 5 presents the main conclusions.

127

128 2. Data and Methods

129 2.1. GEOVIDE data

130 The GEOVIDE cruise was the French contribution to the GEOTRACES program
131 (<http://www.geotraces.org/>) in the North Atlantic. It was carried out on board the French R/V
132 “*Pourquoi Pas?*” from 15 May 2014 to 30 June 2014. A total of 78 stations were measured
133 and sampled along two hydrographic sections: i) the 7th repetition of the OVIDE
134 section (from Portugal to Greenland) and ii) a section across the southern Labrador Sea,
135 between Cape Farewell and Newfoundland. In this paper we only deal with data from the
136 OVIDE section. Because this cruise was inserted in the GEOTRACES project, a large number
137 of parameters were measured, some of them present in the ocean in very low concentration.
138 Therefore, several rosette casts (up to 9) had to be done at some stations; the ~~first~~ **full-depth**
139 cast **with salinity and oxygen samples** was always used as reference for physical
140 characterization of water masses and currents. Stations were named according to the
141 parameters to be measured and the different number of casts to be carried out: Short, Large,
142 XLarge and Super stations. Nearly all the TEIs required by the GEOTRACES program were
143 sampled at XLarge and Super stations, which positions were selected to be representative of
144 the different hydrographic regions, as detailed in section 3.4. Because the ship time was
145 limited to 45 days, the number of stations along the OVIDE section was reduced compared
146 with previous cruises, with 60 stations within 6 weeks during GEOVIDE compared with 95
147 stations usually sampled within about 3 weeks in previous OVIDE cruises. ~~A sensitivity~~
148 ~~analysis was performed with the data from the 2010 OVIDE cruise in order to select the~~
149 ~~station positions and minimize the error associated with the under sampling; as discussed~~
150 ~~later, the main water masses and currents crossing the OVIDE section were correctly sampled~~
151 ~~during the GEOVIDE cruise.~~

152 Conductivity, temperature, pressure and dissolved oxygen were measured using a CTD
153 SBE911 equipped with an SBE-43. The rosette was also equipped with 22 bottles for
154 collecting seawater. For calibration purposes, salinity and oxygen were determined on board
155 from seawater samples, using a salinometer and titration, respectively. The final accuracy was
156 0.001 °C, 0.002, and 2 $\mu\text{mol kg}^{-1}$ for temperature, salinity and oxygen, respectively. Figure 2
157 shows the calibrated temperature, salinity and oxygen measured during CTD-O₂ down casts
158 of the OVIDE section. For more details about the water mass properties and their distributions
159 along the OVIDE section between 2002 and 2012, see García-Ibáñez et al. (2015) and D2016.
160 Finally, the velocities of the upper waters were measured continuously with two ship-mounted

161 ADCP (Ocean Surveyors) at a frequency of 38 Hz and 150 Hz, measuring down to 1000 m
162 and 300 m with vertical resolutions of 24 m and 8 m, respectively.

163 The winter mixed layer depth (WMLD) was estimated along the OVIDE section by visual
164 inspection of the individual potential density and Apparent Oxygen Utilization (AOU)
165 profiles measured during the GEOVIDE cruise. Because the cruise was conducted in summer,
166 the seasonal mixed layer was disregarded and the WMLD was defined as the depth where the
167 slope of the density profile accentuated and the AOU was larger than $0.6 \mu\text{mol kg}^{-1}$. The latter
168 value was chosen because it was the best fit with the density criteria at most stations.

169 **2.2. Inverse model**

170 The absolute geostrophic field orthogonal to the section was estimated by a box inverse model
171 using the hydrographic profiles measured at each station, current measured by the ship
172 mounted ADCP (S-ADCP) and a volume conservation constraint of 1 Sv northward
173 (Lherminier et al., 2007). **For inversion constrain, the S-ADCP data were averaged**
174 **between stations in layers where the shear of the velocity profile was consistent with**
175 **geostrophic velocity profiles.** The inverse model is based on the thermal wind equation and
176 the least-squares formalism following the method described in Mercier et al. (1986) and Lux
177 et al. (2001). Additionally, the Ekman velocities were added to the inverse model: the Ekman
178 transport was estimated from NCEP winds (Kalnay et al., 1996) and equally distributed over
179 the first 30 m. The velocity errors were given by the resulting covariance matrix from the box
180 inverse model. For more details about the inverse model configuration specific to OVIDE, see
181 Lherminier et al. (2007, 2010) and Gourcuff et al. (2011). The volume transports were
182 computed by multiplying velocities by the distances between two stations. Their errors were
183 obtained from the full covariance matrix of velocities, taking into account error correlations,
184 as explained in Mercier (1986).

185 For the computation of transport across the OVIDE section from GEOVIDE data, the first
186 challenge was **to determine the proper** the spatial sub-sampling. **In order to select the**
187 **station positions and minimize the error associated with the sub-sampling, a sensitivity**
188 **analysis was performed with the data from the 2010 OVIDE cruise before the**
189 **GEOVIDE cruise was carried out. The chosen compromise was efficient to represent all**
190 **the main water masses and gave similar AMOC amplitude and consistent transports of**
191 **the currents crossing the section, although the errors on the 2010 regional features**
192 **increased when subsampled. However, in 2014, we used a more precise S-ADCP,**
193 **reducing the S-ADCP error contribution to the inverse model solution. Consequently,**

194 **the final errors of the dynamical structures in 2014 are of the same order of magnitude**
195 **than the errors estimated in previous OVIDE cruises.**

196 ~~In order to evaluate its consequences,~~ The velocities measured by the S-ADCP and those
197 resulting from the inverse model are compared in Fig. 3 (note that the vertical scale differs
198 between the subplots). We see that the inverse model results reproduce the main features of
199 the large-scale circulation captured by the S-ADCP. As expected, mesoscale and ageostrophic
200 structures of horizontal sizes smaller than the distances between stations are visible on the S-
201 ADCP section but are not resolved in the inverse model solution (e.g. between stations 45 and
202 38 or between stations 32 and 27). However, because the geostrophic velocity is an average
203 between stations, this does not imply any bias in the transports. This outcome is also
204 supported by Gourcuff et al. (2011) who, comparing altimetry and S-ADCP data, showed that
205 the contributions of ageostrophic motions tend to cancel out when averaged over the distance
206 between stations.

207 The inverse model estimates the absolute geostrophic transport and the transport of heat and
208 other tracers. The under-sampling of the GEOVIDE cruise notably increases the errors
209 associated with the transport of tracers, because the horizontal gradients of those tracers are
210 less well resolved. The tracer considered in this work is temperature. By applying the
211 GEOVIDE subsampling to the inversion of the OVIDE 2010 data, we estimated a
212 supplementary and independent sampling error of 0.04 PW for heat transport.

213 **2.3. Oceanic database**

214 We used the In Situ Analysis System (ISAS) analysis (Gaillard et al., 2016), which, based on
215 Argo profiles and other qualified *in situ* observations (cruises, fixed-point time series, ships of
216 opportunity, etc.), produced monthly gridded fields of temperature and salinity profiles by
217 optimal interpolation for the period since 2002. We also used EN4 reanalysis. Similar to
218 ISAS, EN4 reanalysis is an optimal interpolation that incorporates *in situ* data measured since
219 1900, filling gaps by extrapolation from the observational data using covariances from the
220 Hadley Centre model (Good et al., 2013). We also used the temperature and salinity analysis
221 developed by JAMSTEC (Hosoda et al., 2008), which is also an optimal interpolation based
222 on Argo profiles, Triangle Trans-Ocean Buoy Network (TRITON) and other *in situ*
223 observations.

224 First, we evaluated the temporal and horizontal extension of the potential temperature (θ) and
 225 salinity (S) anomalies detected in the surface layer from ISAS: both properties were averaged
 226 between 20 and 500 m at each ISAS grid point in the North Atlantic, and monthly anomalies
 227 were then estimated with respect to the 2002–2012 mean values. Second, ISAS, EN4 and
 228 JAMSTEC databases were used to evaluate the heat and freshwater content changes in the
 229 upper 1000 m in the region delimited by 40°–60° N and 45°–10° W: for each month the heat
 230 content (HC_{month}) and the freshwater content (FWC_{month}) of the volume of water in the box
 231 previously defined was estimated following eq. 1 and eq. 2, respectively:

$$232 \quad HC_{month} = \sum_{z=1}^{z=n} \sum_{i=1}^{i=n} \theta_{z,i} * Cp_{z,i} * \rho_{z,i} * V_{z,i} \quad \text{eq. 1}$$

$$233 \quad FWC_{month} = \sum_{z=1}^{z=n} \sum_{i=1}^{i=n} \frac{(35 - S_{z,i}) * V_{z,i}}{35} \quad \text{eq. 2}$$

234 where z and i are the depth levels and grid points of the database, and $Cp_{z,i}$, $\rho_{z,i}$ and $V_{z,i}$ are the
 235 heat content capacity, density and volume of each depth level and grid point of the database.

236 **2.4. Air-sea flux data**

237 In order to evaluate the role of atmospheric forcing on the θ and S anomalies observed during
 238 the GEOVIDE cruise, re-analyzed ERA-Interim data (Berrisford et al., 2011) and NCEP data
 239 (Kanamitsu et al., 2002, <http://www.esrl.noaa.gov/psd/>) were processed. In particular, we
 240 estimated seasonal anomalies of net air-sea heat flux (and its components: sensible heat, latent
 241 heat, net longwave radiation and net shortwave radiation) and freshwater flux (and its
 242 components: precipitation and evaporation) as follows. Firstly, seasonal means were
 243 computed defining winter as DJF, spring as MAM, summer as JJA and autumn as SON.
 244 Secondly, seasonal anomalies were calculated relative to the mean seasonal cycle of 2002–
 245 2012. Finally, the anomalies of winter–spring 2014 that preceded the GEOVIDE cruise were
 246 estimated.

247 Furthermore, the monthly time series of net air-sea heat and freshwater fluxes were used to
 248 evaluate the contribution of the atmospheric forcing to the observed heat and freshwater
 249 content changes in the box defined in section 2.3. Specifically, we integrated net air-sea heat
 250 and freshwater fluxes, **given every 12h/6h in ERA-INTERIM/NCEP, from January 16**
 251 **February 4, 2013 to December 15~~31~~, 2014. The resulting time series were compared with**
 252 **the monthly time series of heat/freshwater content change between one month and the**
 253 **previous month, accumulated from January 2013 to December 2014.**

254

255 3. Results

256 3.1. Circulation across the OVIDE section in 2014

257 The OVIDE section is intersected by permanent currents and gyres that are described by
258 D2016 using the average measurements from the first 6 OVIDE cruises (2002 – 2012). This
259 section presents the intensity, location and extension of these dynamical structures during the
260 GEOVIDE cruise. The results showed hereafter are based on the solution of the inverse model
261 (see Fig. 3b, ~~lower panel~~). Despite the mesoscale structures typical of a single occupation of
262 the section, we can identify and quantify all the main patterns described by D2016.

263 Near Greenland, the ~~Western Boundary Current (WBC)~~ **water** flowings southwestward,
264 guided by the continental slope **is the Western Boundary Current (WBC): it has two**
265 **components, the East Greenland-Irminger Current (EGIC $\sigma_0 < 27.8 \text{ kg m}^{-3}$) and the**
266 **Deep Western Boundary Current (DWBC, $\sigma_0 > 27.8 \text{ kg m}^{-3}$).** During the GEOVIDE
267 cruise, ~~the~~ **its extension of the DWBC** towards the central Irminger Sea at depths $> 2000 \text{ m}$
268 (see Fig. 3b, ~~lower panel~~) is marked by a bottom mesoscale feature typical of the plume
269 structure of the overflow (Spall and Price, 1997). The total intensity of the WBC was
270 estimated at $30.3 \pm 2.1 \text{ Sv}$ southward.

271 The cyclonic gyre defined as the Irminger Gyre (IG) by Våge et al. (2011) can be seen in the
272 western part of the central Irminger Sea. Following their definition, we quantified the
273 intensity of the IG by integrating the northward transport above the isotach 0 m s^{-1} (Fig. 3b),
274 which amounted to $6.8 \pm 3.0 \text{ Sv}$.

275 The Irminger Current (IC) flows northeastwards along the western flank of the Reykjanes
276 Ridge. In 2014, its top to bottom integrated transport amounted to $17.5 \pm 7.3 \text{ Sv}$, which
277 accounts for both, the northward and the southward currents east of the IG. Considering only
278 the northward velocities brings the IC intensity to a value of $22.7 \pm 6.5 \text{ Sv}$.

279 The Eastern Reykjanes Ridge Current (ERRC) flows southwestward east of the Reykjanes
280 Ridge. In 2014, its top-to-bottom integrated transport, between the Reykjanes Ridge and
281 station 34 (Fig. 3), amounted to $13.6 \pm 6.0 \text{ Sv}$ southward.

282 The North Atlantic Current (NAC) at the OVIDE section consists of meandering branches
283 flowing northeastward between the center of the Iceland Basin and the Azores-Biscay Rise

284 (D2016). To determine its horizontal extension, we used the **top-to-bottom volume**
285 **transport accumulated from Greenland to each GEOVIDE station** (the barotropic stream
286 function, (Fig. 4) and the AVISO altimetry data (Fig. 5). The NAC intensity was quantified as
287 the accumulated transport from the relative minimum of the barotropic stream function in the
288 central Iceland Basin up to the maximum of the barotropic stream function in the Western
289 European Basin (D2016). In the Iceland Basin, we found two relative minima of the stream
290 function (Fig. 4) due to the presence of an anticyclonic eddy, which was considered as part of
291 the NAC, as justified in the next section. The limits of the NAC along the OVIDE section are
292 indicated by ~~green-white points~~ **circles** in Fig. 5, between which the different branches of the
293 NAC appear as energetic northeastward currents. The top to bottom intensity of the NAC in
294 2014 amounted to 32.2 ± 11.4 Sv. Following D2016, three different branches of the NAC can
295 be differentiated: the northern branch (**NNAC**), the subarctic front (SAF) and the southern
296 branch (**SNAC**). The SAF is identified as the concomitant intense northward transport and
297 salinity increase around 22.5° W (Fig. 4). In 2014, top-to-bottom transport of the different
298 NAC branches was -0.1 ± 6.4 Sv, 25.0 ± 3.0 Sv and 7.3 ± 54.9 Sv, respectively. Note that the
299 **net transport in the northern branch of the NAC transport is quasibasicly null** with a large
300 associated error and, by contrast, the SAF **bears a very intense central branch** ~~is remarkably~~
301 **large**. This point is discussed in section 4.

302 The easternmost dynamical feature of the OVIDE section is the NAC recirculation. Its
303 intensity of 10.1 ± 6.4 Sv southwestward is determined as the top-to-bottom accumulated
304 transport between the southern limit of the NAC and the easternmost station of the OVIDE
305 section.

306 The intensity of the ~~Meridional Overturning Circulation (AMOC)~~ across the OVIDE section,
307 **referred as MOC hereafter**, was defined from the velocities given by the inverse model as
308 the maximum of the surface to bottom integrated stream function computed in vertical
309 coordinates of potential density referenced to 1000 m (σ_1). During the GEOVIDE cruise, it
310 amounted to 18.7 ± 2.7 Sv and was found at $\sigma_1 = 32.15$ kg m⁻³. Additionally, using the
311 independent monthly MOC index created by Mercier et al. (2015), which is based on
312 altimetry and Argo data, the intensity of the MOC across the OVIDE section amounted to the
313 compatible value of 21.3 ± 1.5 Sv in June 2014, while the 2014 annual mean value of the
314 MOC index was 18.2 Sv.

315 Heat transport during the GEOVIDE cruise was estimated at 0.56 ± 0.06 PW. Following the
316 Bryden and Imawaki (2001) methodology adapted by Mercier et al. (2015) in isopycnal
317 coordinates (**see their equation 1**), we found 0.50 PW transported by the overturning
318 circulation, 0.04 PW by the horizontal or gyre circulation and 0.02 PW by the net transport
319 across the section.

320 **3.2. Fronts and eddies**

321 Together with the above-mentioned permanent circulation features, we observed some
322 remarkable eddies during the GEOVIDE cruise that could modify the “typical” patterns of
323 properties defined by D2016 or García-Ibáñez et al. (2015), **and they as well as it** can affect
324 the distribution of tracers measured during the GEOVIDE cruise.

325 The identification of eddies and fronts was based on the analysis of surface velocities
326 provided by AVISO (see Fig. 5), the velocity profiles given by both the S-ADCP and the
327 inverse model (Fig. 3) and the vertical distribution of properties (Fig. 2). In Fig. 5, we identify
328 clearly that the most energetic currents crossing the OVIDE section are the WBC, close to
329 Greenland, and the NAC with its different branches. Moreover, all the energetic eddies
330 intersecting the OVIDE section were observed in the NAC (Fig. 6) and identified on Fig. 3.
331 From north to south, the first eddy intersecting the section, referred to as the northern eddy, is
332 detected at 56.5° N, 27° W (Fig. 5). This eddy lies between stations 34 and 32 (Fig. 3; Fig. 6),
333 extending from the surface to the bottom but intensified in the upper 600 m. From Fig. 6, we
334 inferred that this eddy was generated in April at approximately 56.5° N, 26° W from the
335 meandering of the NAC north of the OVIDE section; **its position is marked by yellow**
336 **squares in Fig. 6**. In May 2014, the eddy was totally formed and intersected the section
337 between 55.5° N and 57° N. In June 2014, the eddy moved southwestward, in agreement with
338 the general displacement of anticyclonic eddies in the SPNA. The core of the northern eddy,
339 between stations 34 and 32 in Figs. 2a and 2b, shows properties warmer and saltier than the
340 surrounding water, confirming the NAC origin of this eddy; this is why this anticyclonic eddy
341 has been considered as part of the northern branch of the NAC. Note that in May-June, the net
342 transport of this eddy, **from surface to the bottom**, is almost 0 Sv (see Fig. 4 between
343 stations 34 and 32).

344 A large anticyclonic eddy, the central eddy, is observed at 53° N, 26° W, at a tangent to the
345 OVIDE section between stations 30 and 29 (red squares in Fig. 6). However, no signal was
346 detected in the barotropic stream function (Fig. 4) since the northward and southward

347 velocities (Fig. 3a) compensated once integrated between the two stations (Fig. 3b). It is
348 noteworthy that, contrary to the previous anticyclonic eddy, this one is stationary south of the
349 OVIDE section **between March and June** (~~see the monthly evolution in Fig. 6~~) **and was**
350 **found to be quasi-permanent in the altimetry data since 1993 (figure not shown).**
351 Hydrographic properties measured at stations 29 and 30 showed cold and fresh water between
352 350 m and 500 m depth, typical of the Subarctic Intermediate Water (SAIW), which is most
353 likely ~~advected~~**trapped** by this anticyclonic eddy.

354 The most remarkable front present on the OVIDE section is the SAF, associated with the
355 central branch of the NAC. Along the OVIDE section, it is situated between 49.5° N and 51°
356 N in latitude and 23.5° W and 22° W in longitude (red points in Fig. 5 and 6). This front
357 separates cold and fresh water of subpolar origin from warm and salty water of subtropical
358 origin; it is identifiable in Fig. 2 at station 26 by the steep slope of the isotherms and
359 isohalines. The position of this front is known to vary spatially (Bersch 2002; Bower and Von
360 Appen, 2008; Lherminier et al., 2010), creating anomalies of salinity and temperature that will
361 be discussed later.

362 Finally, also in Fig. 5, we identified the southern branch of the NAC with a maximum in the
363 eastward velocities found at 46.5° N, 22° W, ~~just southwest of~~ **GEOVIDE superstation**
364 ~~21 the OVIDE section~~. Despite a very rich mesoscale activity we can distinguish in Fig. 5 that
365 the southern NAC splits into two sub-branches before crossing the OVIDE section, in
366 agreement with D2016. The northernmost sub-branch cuts the section between stations 23 and
367 24 at 48.5° N, 21° W. The southernmost sub-branch evolves into a cyclonic eddy (the
368 southern cyclonic eddy, **light green square in Fig. 6**) that intersects the OVIDE section south
369 of station 21. This eddy is also observed in the velocity profiles (Fig. 3) between stations 21
370 and 19, as well as by the uplifting of isotherms and isohalines in Fig. 2. To its southeast, an
371 anticyclonic eddy (**orange square in Fig. 6**), centered on station 18, marks the southern limit
372 of the NAC and the beginning of the southwestward recirculation. On the OVIDE section, the
373 southern anticyclonic eddy also marks the northwest limit of the presence of Mediterranean
374 Water at about 1000 m depth (Fig. 2b), consistently with its slow westward advection since
375 March (Fig. 6). Note that while the southern anticyclonic eddy (**orange square in Fig. 6**)
376 looks stable over time, the southern cyclonic eddy (**light green square in Fig. 6**) seems more
377 transitory since it is not clearly visible in April.

378 **3.3. Thermohaline anomalies in 2014**

379 The anomalies of potential temperature (θ), salinity (S) and dissolved oxygen along the
380 OVIDE section in 2014 were calculated **on pressure** levels (Fig. 7) **with respect to relative**
381 ~~to the 2002–2012 period (Fig. 7). Note that the~~ **the average of the** six repetitions of the
382 OVIDE section (summers 2002, 2004, 2006, 2008, 2010 and 2012). Only anomalies larger
383 than one standard deviation from the mean are represented in Fig. 7. In the following, S and θ
384 anomalies were quantified as the mean values of the anomaly patches represented in Fig. 7.
385 We identified ~~43~~ different types of anomalies along the OVIDE section. First, negative
386 anomalies in surface-**intermediate** waters were observed **above the WMLD** over the
387 Reykjanes Ridge (**in the IC and the ERRC**) and east of 20° W (**in the SNAC and its**
388 **recirculation**). In the former, the S and θ anomalies were quantified at -0.087 and -1.0495
389 °C, respectively. In the latter, the negative anomalies of S and θ amounted to -0.11 and -0.70
390 °C, respectively. **In the ERRC, negative S and θ anomalies also appeared below the**
391 **WMLD amounting to -0.06 and -0.80 °C, respectively. It concerns a water mass that is**
392 **different from the one in the WMLD; both water masses are separated by a negative**
393 **anomaly of oxygen (Fig. 2c) and a maximum of potential vorticity (not shown).** The
394 cooling and freshening of the surface-intermediate waters were not compensated in density:
395 the cooling dominated and the water was significantly denser (Fig. not shown). Concurrently,
396 a positive oxygen anomaly was observed. ~~All these anomalies are delimited at the bottom by~~
397 ~~the winter mixed layer depth (WMLD, orange line in Fig. 7).~~

398 In both the Irminger Sea and the Iceland Basin, positive anomalies of S and θ were observed
399 in waters deeper than 1000 m. In the Irminger Sea, the S and θ anomalies amounted to 0.017
400 and 0.122 °C, respectively. In the Iceland Basin, they reached similar values, i.e. 0.014 and
401 0.125 °C. In both basins, these anomalies coincided with significant negative oxygen
402 anomalies up to -20 $\mu\text{mol kg}^{-1}$, suggesting that this water mass was not recently ventilated.

403 In the Iberian Abyssal Plain (IAP), negative anomalies of S (-0.12) and θ (-0.67 °C) were
404 observed at the level of the Mediterranean Water (MW), above and below the isopycnal 32.15
405 kg m^{-3} . Although remarkable, those anomalies are difficult to interpret because of the high
406 variability of the Meddy distribution in this area.

407 The displacement of fronts or eddies already identified in the previous section generated other
408 occasional anomalies. The salty and warm anomaly found at 27.4° W, above isopycnal 32.15
409 kg m^{-3} , is explained by the anticyclonic eddy (the northern eddy), which advected water from
410 the NAC. The fresh and cold anomaly localized at 25° W is a consequence of the SAIW

411 brought by the anticyclonic eddy (the central eddy) located at 53° N, 26° W and touching the
412 OVIDE section between stations 30 and 29. Finally, the southeastward displacement of the
413 SAF created a fresh and cold anomaly between 23° W and 22° W because warm and salty
414 North Atlantic Central Water (NACW) usually found in this area was replaced by subpolar
415 water.

416 ~~In Zooming out~~ (Fig. 7c), we found an increase in the ventilation in the first 1000 m, while
417 the deeper waters are less oxygenated when compared to the 2002–2012 period. Remarkably,
418 **The anti-correlation between the oxygen anomalies are anti-correlated with and the θ -S**
419 **anomalies will be discussed in section 4.2.**

420 **3.4. Settling the special GEOVIDE stations in the framework of the large-scale and** 421 **mesoscale circulation**

422 As part of the GEOTRACE program, seven superstations and three XLarge stations were
423 carried out along the OVIDE section in 2014 **for sampling TEIs in the SPNA. The TEIs**
424 **results will be published in this Biogeoscience GEOVIDE Special Issue (e.g. Cossa et al.,**
425 **2017, about mercury; Lemaître et al., 2017, about particulate barium; Le Roy et al., in**
426 **prep., about radium 226; Tonnard et al., in prep., about dissolved iron). In order to**
427 **facilitate the interpretation of the TEIs distribution,** here, we contextualize the
428 superstations and XLarge stations (red and green numbers, respectively, in Figs. 2, 3 and 4,
429 and pink stars in Fig. 5) in the physical framework described above. Apart from station 26,
430 which was specifically selected in real-time in the middle of the SAF, and station 38 over the
431 Reykjanes Ridge, all the other special stations are representative of relatively large
432 hydrographic domains since they are not strongly affected by the peculiar mesoscale features
433 described in section 3.2.

434 Specifically, from Greenland to Portugal, these stations were located in: the East Greenland
435 Coastal Current (EGCC, station 53), the East Greenland-Irminger Current (EGIC, station 60,
436 same position than 51), the Irminger Gyre (station 44, same position than station 46), in the
437 middle of the Iceland Basin (being part of the NNAC ~~northern branch~~, station 32), in the
438 SNAC ~~southern branch~~ (station 21), in the center of the southward recirculation in the IAP
439 (station 13), on the Iberian Peninsula slope (station 8) and, finally, on the Portuguese
440 continental shelf (station 2). Importantly for the GEOTRACES community, although the
441 superstations and XLarge stations are representative in terms of circulation, the large-scale S–

442 θ anomalies detailed in section 3.4 need to be taken into account when comparing GEOVIDE
443 data with data from the previous decade.

444

445 **4. Discussion**

446 **4.1. State of the circulation during the GEOVIDE cruise with respect to the** 447 **mean state**

448 We will first discuss the circulation patterns seen during the GEOVIDE cruise in comparison
449 with the mean position, extension and intensity of the main currents intersecting the OVIDE
450 section defined by D2016. Despite the coarse resolution of the GEOVIDE stations, all the
451 circulation structures are identified in the inverse model solution (Table 1). The intensity of
452 the WBC and the IG are similar to the mean state with a quite high reliability (low relative
453 error). The transports of the ERRC and the southwestward recirculation in the IAP are also
454 very similar to the mean state, but remained to a large degree uncertain. Conversely, the IC
455 and NAC are different from the mean state, but not significantly.

456 **When defining the IC as in D2016, we saw an increase in the IC intensity in 2014, but**
457 **within the observed variability (Table 1). However, the such-defined IC encompasses a**
458 **warm and salty northward transport and a cold and fresh southward transport. So, to**
459 **go further in the analysis of IC, we compared its northward component near Reykjanes Ridge**
460 **with its equivalent from the 2002–2012 mean data (not shown in D2016). In this case, the IC**
461 **amounted to 22.7 ± 6.5 Sv, which is significantly larger than the northward IC computed from**
462 **D2016 data: 11.0 ± 3.4 Sv. Our result is similar to the estimate of Väge et al. (2011) who**
463 **quantified the IC at 19 ± 3 Sv (1991–2008). Therefore, we conclude that the thus-defined IC**
464 **was strengthened in 2014 in relation with respect to the 2002–2012 mean value. Note that the**
465 **northward component of the IC, between stations 38 and 41, transports water masses that are**
466 **warmer and saltier than those advected southward, between stations 41 and 45, (Fig. 2); so,**
467 **the intensification of the Irminger Current is meaningful in terms of transport of warm and**
468 **salty water to the north, and actually contributes to the upper limb of the MOC (Fig. 4, dotted**
469 **line).**

470 Concerning the weaker NAC, its 2014 intensity, 32.2 ± 11.4 Sv, is weaker although within
471 the limits of the observed variability (41.8 ± 3.7 Sv). in 2014, By the decomposition of this
472 wide current, it is very likely that the difference comes from the change in the intensity of

473 the northern branch of the NAC: -0.1 ± 6.4 Sv was computed in GEOVIDE, while 11.0 ± 3.0
474 Sv was estimated by D2016. ~~However, We believe that~~ the weakening of the northern branch
475 of the NAC in 2014 was **partially compensated** ~~due the high mesoscale activity along the~~
476 ~~Maury Channel in the Iceland Basin (Fig. 5), with anticyclonic eddies flowing southwestward~~
477 ~~that temporarily blocked the northeastward propagation of the northern branch of the NAC. It~~
478 ~~is possible that part of the current was deflected westward into the intensified Irminger~~
479 ~~Current. However, we noticed that the intensity by the~~ **doubling of transport** of the NAC
480 central branch of the NAC, **when** ~~simultaneously nearly doubled in 2014 compared with the~~
481 2002–2012 mean (25 ± 3 Sv vs. 14 ± 6 Sv), suggesting there was ~~also~~ a partial transfer of
482 transport from the northern to the central branch of the NAC.

483 The SAF, that bears the central branch of the NAC, shows also a remarkable southeastward
484 displacement in 2014 ~~in relation with respect~~ to the mean circulation pattern (**station 26 in**
485 Fig. 1), of about 100 km. **A careful study of the ADT streamlines (Fig. 8) showed that this**
486 **displacement was not due to a peculiar meandering of the front and that the SAF was**
487 **actually narrower and located more to the southeast in 2014, when compared to the**
488 **2002-2012 mean.** ~~In March 2014, Grist et al. (2015) also detected a southward displacement~~
489 ~~of the NAC along the 30° W meridian by the analysis of EN4 data. However, it should be~~
490 ~~noted that their result concerns a more southern branch of the NAC (41° N) that does not~~
491 ~~cross the OVIDE section and recirculates southward in the Azores Current (Fig. 1).~~ **Bersch et**
492 **al. (2007) linked the northwestward displacement of the SAF in the eastern North**
493 **Atlantic in the late 1990's to a shift from positive to negative values in the index of the**
494 **North Atlantic Oscillation (NAO), which is the dominant mode of atmospheric**
495 **variability over the North Atlantic. After a decade of neutral values, the winter NAO**
496 **index turned positive in 2011 and continued positive in 2013 and 2014 (Hurrell et al.,**
497 **2017). The southeastward displacement of the SAF is thus symmetric to Bersch et al.**
498 **(2007) and consistent with their observations.**

499 ~~Moreover, D2016 also defined~~ **Along the OVIDE section,** some permanent circulation
500 features **were observed by D2016,** where the velocity was found to be in the same direction
501 for all repeated measures ~~on the OVIDE section over the~~ 2002–2012 **period** (see their Fig. 4).
502 In our Fig. 3, we found most of these permanent circulation features: the WBC, IC, ERRC,
503 two deep southward veins transporting the **Iceland-Scotland Overflow Water (ISOW)** in the
504 Iceland Basin, and the northward transport over Eriador Seamount in the intermediate layer.
505 Only the “permanent” anticyclonic eddy marking the southern limit of the NAC moved: it

506 was expected between station 20 and 21 according to the mean circulation (Fig. 1), but was
507 instead found at station 18, i.e. more to the southeast, during the GEOVIDE cruise (and called
508 the southern anticyclonic eddy previously).

509 The inverse model solution also provides a robust estimate of both the intensity of the MOC
510 and the heat transport. We observed a heat transport of 0.56 ± 0.06 PW. To compare it with
511 the 2002–2010 average, we used the data of Mercier et al. (2015), without data from 1997,
512 **because it did not belong to our reference period**, and obtained 0.47 ± 0.05 PW. Even if the
513 2014 value is not statistically different from the mean, it is surprising to find such a high heat
514 transport considering the cold anomaly observed in the NAC surface waters (Fig. 7). To
515 determine the role of the MOC in this result, we first looked at the 2014 MOC (18.7 ± 2.7 Sv),
516 which is 2.5 Sv higher than the 2002–2010 average (16.2 ± 2.4 Sv). Note that including 2012
517 data (15 Sv and 0.39 PW, not published) in the mean increases the difference with 2014. **This**
518 **result is in line with the observation of Rossby et al. (2017), who found that the MOC**
519 **intensity at 59.5 °N was larger for the period from late-2012 to early-2016 than the**
520 **average over 1993–2016.** To improve our quantification of the influence of the MOC on heat
521 transport, we used the heat transport proxy HT^* built by Mercier et al. (2015), which
522 evaluates the heat transport only driven by the diapycnal circulation, known to be the
523 dominant term of heat transport for all the OVIDE cruises. The proxy (eq. 3) is based on the
524 MOC intensity (MOC_σ) and the temperature difference between the upper and lower limbs of
525 the MOC (ΔT):

$$526 \quad HT^* = \rho \cdot c_p \cdot \Delta T \cdot MOC_\sigma \quad (\text{eq. 3})$$

527 where HT^* , ρ and c_p are the heat transport proxy, the *in situ* density and the specific heat
528 capacity, respectively. During GEOVIDE, HT^* amounted to 0.49 PW, with $MOC_\sigma = 18.7$ Sv
529 and $\Delta T = 6.40$ °C. The 2002–2010 mean values of HT^* , MOC_σ and ΔT were 0.43 PW, 16.2
530 Sv and 6.79 °C, respectively. So, the heat transport index and MOC_σ were larger in 2014 than
531 the mean values, while the ΔT was smaller, which is consistent with the cold anomaly. These
532 results show that the larger MOC_σ measured during GEOVIDE was enough to compensate for
533 the heat transport decrease due to the cooling of the surface waters. This result **might be the**
534 **effect of a short-term variability since it** contrasts with the study of Desbruyères et al.
535 (2015), who argued that the long-term variability of the ocean heat transport at the OVIDE
536 section is dominated by the advection by the mean velocity field of temperature anomalies
537 formed upstream rather than the velocity anomalies acting on temperature.

538 **4.2. Negative anomalies of θ and S in surface-intermediate layers explained by the local**
539 **atmospheric forcing.**

540 **The long-term evolution of heat content anomaly with respect to the 2002–2012 mean**
541 **(Fig. 9) was calculated in the upper 1000m over the SPNA region delimited by 40–60 °N**
542 **latitude and 45–10 °W longitude (green square in Fig. 11). As shown by Robson et al.**
543 **(2016), the SPNA started a new long-term cooling period since the mid-2000s. By**
544 **analyzing outputs of coupled climate models, Robson et al. (2017) argued that this new**
545 **cooling period is led by the reduced ocean heat transport convergence resulting from a**
546 **long term slow-down of the AMOC. Within this long-term cooling period, we will focus**
547 **hereafter on the pronounced heat content drop that happened between 2013 and 2014.**

548 The negative anomalies of θ and S in the surface-intermediate layers along the OVIDE
549 section in May–June 2014 **with respect to the mean 2002–2012** were actually present over
550 the whole of the year 2014 and the whole SPNA (Fig. 8**10**). θ and S anomalies in the ocean
551 can be caused by changes in the lateral advection of water masses with different properties,
552 and/or by anomalous net air-sea fluxes. **Considering the high ocean heat transport**
553 **observed during GEOVIDE, we analyzed the air-sea flux anomalies.** The mean winter–
554 spring (W-S 2014) anomalies of air-sea heat flux presented strong negative anomalies over
555 the whole SPNA (Fig. 119a), i.e. the ocean lost more heat than ~~usual~~ **the 2002–2012 average,**
556 with contribution of **both** sensible and latent air-sea heat fluxes (Fig. 119b and 119c). **The**
557 **spatial repartition of the freshwater budget is mainly driven by the patterns of the**
558 **precipitation anomalies, with a net freshwater loss southwest of the region and a clear**
559 **gain in the eastern side.** ~~The high latent heat loss is associated with high evaporation, which~~
560 ~~can be seen in Fig. 9e.~~ **When the net freshwater flux was integrated over our region (Fig.**
561 **12), the net freshwater gain (Fig. 119d) shows that high precipitation rates (Fig. 119f)**
562 **overcame the freshwater loss by evaporation (Fig. 11e).** These anomalous air-sea heat and
563 freshwater fluxes in the eastern SPNA suggest that the negative θ and S anomalies observed
564 in the surface-intermediate waters during GEOVIDE were **mainly** formed locally by
565 atmospheric forcing.

566 The heat/freshwater content changes in the upper 1000 m of the ocean during the 2013–2014
567 period were evaluated together with the air-sea heat/freshwater fluxes in ~~a~~ **the region in the**
568 ~~eastern SPNA~~ delimited by 40–60 °N latitude and 45–10 °W longitude. In agreement with
569 Grist et al. (2015), we found that the air-sea heat flux is the main responsible for the cooling

570 observed in the surface-intermediate layers. Exactly, we estimated the accumulated air-sea
571 heat loss from summer 2013 to summer 2014 at 6.8×10^{21} J, while the accumulated ocean heat
572 loss for the same period amounted to 4.8×10^{21} J (averaged of ISAS, EN4 and JAMSTEC
573 estimates). **This result is also in agreement with the findings of Dutchez et al. (2016), who**
574 **argued the 2013–2015 intense air-sea heat fluxes drove water masses transformation,**
575 **which is an irreversible process. Recently, Frajka-Williams et al. (2017) explained that**
576 **such short-term cooling is mainly caused by the atmospheric forcing since the**
577 **hypothetical slow-down of the AMOC would take longer to generate a cooling of this**
578 **magnitude. Moreover,** Concerning the freshwater, we detected that, despite the variability
579 in freshwater content change at intra-seasonal and seasonal time-scales (Fig. 12a), there is a
580 good agreement between the trends shown by the ocean freshwater content and the air-sea
581 freshwater flux over the 2013–2014 period. **We are aware of the large uncertainty**
582 **associated with the air-sea freshwater flux (Josey and Marsh, 2005; Dee et al., 2011) and**
583 **the ocean freshwater content. Therefore, we estimated both variables from two and**
584 **three databases, respectively. The difference between the ERA-Interim and NCEP**
585 **estimates of accumulated air-sea freshwater flux over the two years amount to 0.4×10^{12}**
586 **m³, while the ocean freshwater content estimates differ by 0.3×10^{12} m³ (Fig. 12). We**
587 **conclude that between 70 % and 100 % of the freshening observed in the considered**
588 **volume of the SPNA is caused by air-sea freshwater inputs.** These results support our
589 conclusion that the negative θ and S anomalies observed in the surface-intermediate waters
590 during the GEOVIDE cruise were locally formed by atmospheric forcing. ~~The dominant role~~
591 ~~of the air-sea heat flux over the changes of ocean heat content contrasts with the results of~~
592 ~~several studies that showed that the heat content variability in the SPNA is mainly controlled~~
593 ~~by oceanic heat transport variability (e.g. Hátún et al., 2005; Marsh et al., 2008; Desbruyères~~
594 ~~et al., 2015).~~

595 More evidence for the important role of air-sea fluxes is provided by the distribution of θ , S
596 and oxygen anomalies in the water column. Indeed, the WMLD along the OVIDE section east
597 of the Reykjanes Ridge 20° W coincided with the deep limit of the anomalies most of the time
598 (Fig. 7). **It is somewhat more complex in the ERRC, where the WMLD crosses the**
599 **anomaly separating Subpolar Mode Water (SPMW) and upper Labrador Sea Water**
600 **(LSW), see Fig. 2b; both water masses were advected together by the ERRC, but**
601 **probably issued from different ventilation regions. According to de Boisséson et al.**
602 **(2012), the SPMW is formed by air-sea interactions on its way around the Iceland basin.**

603 The sign of **all** the anomalies **described above** is consistent with vertical mixing in the winter
604 before the GEOVIDE cruise, transferring the cold, fresh and oxygenated anomalies imprinted
605 locally by the atmosphere into the whole mixed layer. **In the Irminger Sea** Remarkably, the
606 **WMLD** ~~orange line~~ in Fig. 7 reaches 1200 m ~~in the Irminger Sea although~~ while deep
607 convection did not exceed 700 m in winter 2014 in the central Irminger Sea (Piron, 2015;
608 Duchez et al., 2016). It most likely results from the advection in the depth range 700–1200 m
609 of high-oxygen intermediate water with densities slightly denser than the water above and
610 possibly formed south of Greenland, as suggested by Fig. 5.3 of Piron (2015).

611 Below the orange line in Fig. 7, we observed mainly warming, salinification and
612 deoxygenation. This is in agreement with the tendencies observed since 2002 along the
613 OVIDE section. Deep waters below 1300 m depth in the Irminger Sea were obviously not
614 recently renewed, apart from the plume of DSOW. Kieke and Yashayaev (2015) showed the
615 evolution of S and θ in the LSW measured in the Labrador Sea: below 1300 m, the positive
616 tendencies of S and θ were similar to those observed in the Irminger Sea, and concerned the
617 dense LSW formed in the 1990s.

618 ~~Negative S anomalies of the surface waters of the SPNA were observed in the 1970s, during~~
619 ~~the Great Salinity anomaly event, and were explained by a larger pulse of freshwater getting~~
620 ~~into the SPNA through the Denmark Strait (Dickson et al. 1988; Robson et al., 2014).~~
621 ~~Concurrently, the SPG started a cool phase that persisted up to the beginning of the 1990s and~~
622 ~~was explained by the decrease in the ocean heat transport convergence with a minor~~
623 ~~contribution of atmospheric forcing (Williams et al., 2014; Robson et al., 2014). Later, from~~
624 ~~mid-1990s to mid-2000s, positive anomalies of θ and S in the surface waters of the SPNA~~
625 ~~were observed, coinciding with the contraction and weakening of the SPG (e.g. Bersch, 2002;~~
626 ~~2007; Sarafanov et al., 2008; Häkkinen et al., 2011). In the introduction, we detailed the~~
627 ~~different hypotheses postulated by different authors to explain these anomalies, all of whom~~
628 ~~interpreted the anomalies as originating in the Labrador Sea. Similarly, Hermanson et al.~~
629 ~~(2014), by analyzing three versions of the Met Office Decadal Prediction System, identified~~
630 ~~the three periods of cooling-warming of the SPNA indicated above: cooling from the~~
631 ~~beginning of the 1970s, warming from mid-1990s to mid-2000s, and cooling from 2014, with~~
632 ~~the latter predicted to continue at least up to 2017 and recently confirmed by data (Piron et al.,~~
633 ~~2017; Yashayaev and Loder, 2017). For these three events, the authors found that the~~

634 ~~mechanism controlling the anomalies was the heat convergence related to changes in MOC~~
635 ~~intensity.~~

636 ~~The 2014 anomaly was the first detected, after approximately 18 years of warming and~~
637 ~~salinification. The winter NAO index for winter 2014 was positive and high (0.92), so,~~
638 ~~following Bersch et al. (2007), an expansion of the subpolar gyre (SPG) would be expected.~~
639 ~~Although we observed a southward displacement of the SAF in 2014, we could not prove the~~
640 ~~link between the probable expansion of the SPG and the advection of additional subpolar~~
641 ~~water northeastward. By contrast, we showed that the cooling and freshening of the surface-~~
642 ~~intermediate waters observed in summer 2014 were locally formed in the eastern SPNA by~~
643 ~~the atmospheric forcing.~~

644

645 **5. Summary and conclusions**

646 This paper addresses two main issues: first, under the umbrella of the GEOTRACES program,
647 it contextualizes the physical background of the GEOVIDE cruise carried out in May–June
648 2014, which is essential for the interpretation of distribution of TEIs in the eastern SPNA.
649 Second, it elucidates the cause of the cold and fresh anomaly detected in the surface waters of
650 the eastern SPNA in May–June 2014.

651 Concerning the circulation across the OVIDE sections, the most important difference between
652 the GEOVIDE state and the 2002–2012 mean state defined by D2016 is a strengthened
653 Irminger Current and a weaker North Atlantic Current, with a possible transfer of volume
654 transport from its northern branch to ~~both its central branch and the Irminger Current~~. The
655 intensity of the MOC was the highest measured at the OVIDE section since 2002, 18.7 ± 3.0
656 Sv, and was high enough to compensate the negative temperature anomaly detected in the
657 surface waters, resulting in a high heat transport across the OVIDE section, 0.56 ± 0.06 PW.

658 The special GEOVIDE stations where the trace elements were measured were indeed
659 representative of the targeted hydrographic regions, away from the core of the main
660 advected eddies identified along the sections. Nevertheless some precautions should be taken
661 when comparing with previous years since temperature, salinity and oxygen of the SPNA
662 winter mixed layer in 2014 were significantly different from the 2002–2012 mean.

663 Finally, we demonstrated that the cold and fresh anomalies in the 2014 mixed layer induced
664 consistent changes in heat and freshwater content of the SPNA. **This strong 2013–2014**
665 **cooling is inserted in a long-term cooling in the SPNA that started in mid–2000s.** Our
666 results elucidate the important role of air-sea flux in the θ -S changes in this region **at short**
667 **time-scale**, overcoming the warming ~~and salinification~~ induced by the increase in the MOC
668 amplitude and associated heat transport **in May–June 2014.**

669

670 **Acknowledgements**

671 We gratefully acknowledge the crew of the *Pourquoi Pas?* vessel for their help and assistance
672 during the cruise and for winch repairs. We also acknowledge the work of the UTM-CSIC
673 (Spain) technical staff for the CTD manipulation. The GEOVIDE cruise would not have been
674 achieved without the technical skills and the commitment of Catherine Kermabon, Pierre
675 Branellec, Philippe Le Bot, Olivier Ménage, Stéphane Leizour, Michel Hamon and Floriane
676 Desprez de Gésincourt (LOPS) and also Fabien Péroult and Emmanuel de Saint Léger
677 (CNRS). We are particularly grateful to Dr Géraldine Sarthou for her persistent dedication to
678 the project and her precious advices, and to the three anonymous reviewers who greatly
679 helped us in improving the manuscript. The NCEP Reanalysis 2 data were provided by the
680 NOAA/OAR/ESRL PSD, Boulder, Colorado, USA, from their web site at
681 <http://www.esrl.noaa.gov/psd/>. The altimeter products were produced by Ssalto/Duacs and
682 distributed by Aviso with support from CNES.

683 For this work, P. Zunino was supported by CNRS and IFREMER, within the framework of
684 the projects AtlantOS (European Union’s Horizon 2020, grant N° 633211) and GEOVIDE
685 (ANR-13-BS06-0014-02), respectively. H. Mercier was financed by CNRS, P. Lherminier by
686 Ifremer and N. Daniault by the University of Western Brittany, Brest. M.I. García-Ibáñez and
687 F.F. Pérez were supported by the Spanish Ministry of Economy and Competitiveness through
688 the BOCATS (CTM2013-41048-P) project co-funded by the Fondo Europeo de Desarrollo
689 Regional 2014–2020 (FEDER).

690

691

692 **References**

693 *Barrier, N., Deshayes, J., Treguier, A. M. and Cassou, C.: Heat budget in the North Atlantic subpolar*
694 *gyre: Impacts of atmospheric weather regimes on the 1995 warming event, Progress in*
695 *Oceanography, 130, 75-90, [doi:10.1016/j.pocean.2014.10.001](https://doi.org/10.1016/j.pocean.2014.10.001), 2015*

696 *Berrisford, P., Kallberg, P., Kobayashi, S., Dee, D., Uppala, S., Simmons, A.J., Poli, P., Sato, H.:*
697 *Atmospheric conservation properties in ERA-Interim, Q. J. R. Meteorol. Soc. 137, 1381–1399.*
698 *DOI:10.1002/qj.864, 2011.*

699 *Bersch, M., North Atlantic Oscillation-induced changes of the upper layer circulation in the northern*
700 *North Atlantic Ocean, J. Geophys. Res.-Oceans, 107(C10), 3156, [doi:10.1029/2001JC000901](https://doi.org/10.1029/2001JC000901), 2002*

701 *Bersch, M., Yashayaev, I., Koltermann, K. P.: Recent changes of the thermohaline circulation in the*
702 *subpolar North Atlantic, Ocean Dynamics, 57:223–235, doi:10.1007/s10236-007-0104-7, 2007.*

703 **de Boissésou, E., Thierry, V., Mercier, H., Caniaux, G., and Desbruyères, D.: Origin, formation and**
704 **variability of the Subpolar Mode Water located over the Reykjanes Ridge, Journal of Geophysical**
705 **Research, 117, C12005, doi:10.1029/2011JC007519, 2012.**

706

707 *Bower, A. S. and von Appen, W.J.: Interannual variability in the pathways of the North Atlantic current*
708 *over the Mid-Atlantic Ridge and the impact of topography, J. Phys. Oceanogr., 38(1), 104–120,*
709 *doi:10.1175/2007JPO3686.1, 2008.*

710 *Bryden, H. and Imawaki, S.: Ocean heat transport, in: Ocean Circulation and Climate, edited by:*
711 *Siedler, G., Church, J., and Gould, J., Academic Press, 2001.*

712 **Cossa, D., Heimbürger, L-E., Pérez, F. F., García-Ibáñez, M.I., Sonke, J. E., Planquette, H. ,**
713 **Lherminier, P., Sarthou, G.: Mercury distribution and transport in the North Atlantic Ocean along**
714 **the Geotraces-GA01 transect, Biogeosciences Discuss., doi:10.5194/bg-2017-467, 2017.**

715 *Daniault, N., Mercier, H., Lherminier, P., Sarafanov, A., Falina, A., Zunino P., Pérez, F. F., Rios, A. F.,*
716 *Ferron, B., Huck, T., Thierry, V., Gladyshev, S.: The northern North Atlantic Ocean mean circulation in*
717 *the early 21st Century, Progress In Oceanography , 146, 142-158, doi:10.1016/j.pocean.2016.06.007,*
718 *2016.*

719 *Desbruyères, D., Mercier, H., Thierry, V.: On the mechanisms behind decadal heat content changes in*
720 *the eastern subpolar gyre, Progress in Oceanography, 132, 262–272,*
721 *doi:10.1016/j.pocean.2014.02.005, 2015.*

722 *Deshayes, J., and Frankignoul, C.: Simulated variability of the circulation in the North Atlantic from*
723 *1953 to 2003. J. Climate, 21, 4919–4933, doi:10.1175/2008JCLI1882.1, 2008.*

724 *Dickson, R.R., Meincke, J., Malmberg, S.A., Lee, A.J.: The “great salinity anomaly” in the northern*
725 *north Atlantic 1968–1982, Prog. Oceanogr., 20 (2), 103–151, doi: 10.1016/0079-6611(88)90049-3,*
726 *1988.*

727 *Duchez, A., Frajka-Williams, E., Josey, S. A., Evans, D. G., Grist, J. P., Marsh, R., McCarthy, G. D., Sinha,*
728 *B., Berry, D. I., and Hirschi, J. J-M: Drivers of exceptionally cold North Atlantic Ocean temperatures*
729 *and their link to the 2015 European heat wave, Environ. Res. Lett., 11, doi:10.1088/1748-*
730 *9326/11/7/074004, 2016.*

731 **Frajka-Williams, E., Beaulieu, C., Duchez, A.: Emerging negative Atlantic Multidecadal Oscillation**
732 **index in spite of warm subtropics, Scientific Reports, doi:10.1038/s41598-017-11046-x, 2017.**

733

734 *Gaillard, F., Reynaud, T., Thierry, V., Kolodziejczyk, N., Von Schuckmann, K.: In Situ–Based Reanalysis*
735 *of the Global Ocean Temperature and Salinity with ISAS: Variability of the Heat Content and Steric*
736 *Height, Journal of Climate, doi:10.1175/JCLI-D-15-0028.1, 2016*

737 *García-Ibáñez, M. I., Pardo, P. C., Carracedo, L. I., Mercier, H., Lherminier, P., Ríos, A. F., and Pérez, F.*
738 *F.: Structure, transports and transformations of the water masses in the Atlantic Subpolar Gyre, Prog.*
739 *Oceanogr., 135, 18–36, doi:10.1016/j.pocean.2015.03.009, 2015.*

740 **García-Ibáñez, M. I., Pérez, F. F., Lherminier, P., Zunino, P., Tréguer, P.: Water mass distributions**
741 **and transports for the 2014 GEOVIDE cruise in the North Atlantic, Biogeosciences Discuss.,**
742 **doi:10.5194/bg-2017-355, 2017.**

743

744 Good, S.A., Martin, M.J. and Rayner, N. A.: EN4: quality controlled ocean temperature and salinity
745 profiles and monthly objective analyses with uncertainty estimates. *J Geophys Res.*, 118, 6704– 6716,
746 doi:10.1002/2013JC009067, 2013.

747 Gourcuff, C., Lherminier, P., Mercier, H., and Le Traon, P. Y.: Altimetry Combined with Hydrography
748 for Ocean Transport Estimation, *J. Atmospheric Ocean. Technol.*, 28(10), 1324–1337,
749 doi:10.1175/2011JTECHO818.1, 2011.

750 Grist, J. P., Josey, S. A., Jacobs, Z. L., Marsh, R., Sinha, R., Sebille, E. V. : Extreme air–sea interaction
751 over the North Atlantic subpolar gyre during the winter of 2013–2014 and its sub -surface legacy,
752 *Clim Dyn*, doi:10.1007/s00382-015-2819-3, 2015.

753 ~~Häkkinen, S., Rhines, P. B.: Decline of subpolar North Atlantic circulation during the 1990s, *Science*, 304,~~
754 ~~555–559, 2004~~

755 Häkkinen, S., Rhines, P. B., and Worthen, D. L.: Warm and saline events embedded in the meridional
756 circulation of the northern North Atlantic. *J. Geophys. Res.*, 116, C03006, doi:10.1029/2010JC006275,
757 2011.

758 Hátún, H., Sandø, A.B., Drange, H., Hansen, B., and Valdimarsson, H.: Influence of the Atlantic
759 subpolar gyre on the Thermohaline circulation. *Science*, 309, 1841–1844,
760 doi:10.1126/science.1114777, 2005.

761 ~~Herbaut, C., and Houssais, M. N.: Response of the eastern North Atlantic subpolar gyre to the North~~
762 ~~Atlantic Oscillation, *Geophys. Res. Lett.*, 36, L17607, doi:10.1029/2009GL039090, 2009.~~

763 Hermanson, L., Eade, R., Robinson, N. H., Dunstone, N. J., Andrews, M. B., Knight, J. R., Scaife, A. A.,
764 and Smith, D. M.: Forecast cooling of the Atlantic subpolar gyre and associated impacts, *Geophys.*
765 *Res. Lett.*, 41, 5167–5174, doi:10.1002/2014GL060420, 2014.

766 Holliday, N. P., Cunningham, S. A., Johnson, C., Gary, S. F., Griffiths, C., Read, J. F., and Sherwin, T.:
767 Multidecadal variability of potential temperature, salinity, and transport in the eastern subpolar
768 North Atlantic, *J. Geophys. Res. Oceans*, 120, 5945– 5967, doi:10.1002/2015JC010762, 2015.

769 Hosoda, S., Ohira, T. and Nakamura, T.: A monthly mean dataset of global oceanic temperature and
770 salinity derived from Argo float observations, *JAMSTEC Rep. Res. Dv.*, 8, 47- 59, 2008.

771

772 **Hurrell, James & National Center for Atmospheric Research Staff (Ed). Last modified 06 Oct 2017.**
773 **“The Climate Data Guide: Hurrell North Atlantic Oscillation (NAO) Index (station-based)”.**
774 **[https://climatedataguide.ucar.edu/climate-data/hurrell-north-atlantic-oscillation-nao-index-](https://climatedataguide.ucar.edu/climate-data/hurrell-north-atlantic-oscillation-nao-index-stationèbased)**
775 **[stationèbased](https://climatedataguide.ucar.edu/climate-data/hurrell-north-atlantic-oscillation-nao-index-stationèbased).**

776

777 IPCC, 2007: *Climate Change 2007: The Physical Science Basis. Contribution of Working Group I to the*
778 *Fourth Assessment Report of the Intergovernmental Panel on Climate Change [Solomon, S., D. Qin, M.*
779 *Manning, Z. Chen, M. Marquis, K.B. Averyt, M. Tignor and H.L. Miller (eds.)]. Cambridge University*
780 *Press, Cambridge, United Kingdom and New York, NY, USA, 996 pp.*

781
782 Johnson, G. C., Lyman, J. M., Boyer, T., Domingues, C. M., Ishii, M., Killick, R., Monselesan, D., and
783 Wijffels, S. E.: Ocean heat content [in “State of the Climate in 2015”]. *Bull. Amer. Meteor. Soc.*, 97 (8),
784 S64–S65, 2016.

785 Josey, S. A., and Marsh, R.: Surface freshwater flux variability and recent freshening of the North
786 Atlantic in the eastern subpolar gyre, *Journal of Geophysical Research*, VOL. 110, C05008,
787 doi:10.1029/2004JC002521, 2005.

788
789 Kalnay, E., Kanamitsu, M., Kistler, R.: The NCEP/NCAR 40-year reanalysis project. *Bulletin of the*
790 *American Meteorological Society* 77, 437–470, 1996

791
792 Kanamitsu, M., Ebisuzaki, W., Woollen, J., Yang, S.-K., Hnilo, J. J., Fiorino, M., and Potter, G.L.: NCEP–
793 DOE AMIP-II Reanalysis (R-2). *Bulletin of the American Meteorological Society* 83:1631–1643, 2002.

794 Kieke, D. and Yashayaev, I.: Studies of Labrador Sea Water formation and variability in the subpolar
795 North Atlantic in the light of international partnership and collaboration, *Progress in Oceanography*,
796 132, 220–232, doi:10.1016/j.pocean.2014.12.010, 2015.

797 Khatiwala, S., Tanhua T., Mikaloff Fletcher S., Gerber M., Doney S.C., Graven H. D., Gruber N.,
798 McKinley G.A., Murata A., Rios A.F. and Sabine C.L.: Global ocean storage of anthropogenic carbon.
799 *Biogeosciences*, 10, 2169–2191, doi:10.5194/bg-10-2169-2013 ,2013

800 Kuhlbrodt, T., Griesel, A., Montoya, M., Levermann, A., Hofmann, M., and Rahmstorf, S.: On the
801 driving processes of the Atlantic meridional overturning circulation, *Rev. Geophys.*, 45, RG2001,
802 doi:10.1029/2004RG000166, 2007. **Discuss.**

803 **Lemaître, N., Planquette, H., Planchon, F., Sarthou, G., Jacquet, S., García-Ibáñez, M.I, Gourain, A.,**
804 **Cheize, M., Monin, L., André, L., Laha, P., Terryn, H., Dehairs, F. : Particulate barium tracing**
805 **significant mesopelagic carbon remineralisation in the North Atlantic, *Biogeosciences***
806 ***Discuss.*, doi:10.5194/bg-2017-400, 2017.**

807 Lherminier, P., Mercier, H., Gourcuff, C., Alvarez, M., Bacon, S., and Kermabon, C.: Transports across
808 the 2002 Greenland-Portugal Ovide section and comparison with 1997, *J. Geophys. Res.*,
809 112(C07003), doi:10.1029/2006JC003716, 2007.

810 Lherminier, P., Mercier, H., Huck, T., Gourcuff, C., Pérez, F. F., Morin, P., Sarafanov, A., and Falina, A.:
811 The Atlantic Meridional Overturning Circulation and the subpolar gyre observed at the A25-OVIDE
812 section in June 2002 and 2004, *Deep-Sea Res. Part -Oceanogr. Res. Pap.*, 57(11), 1374–1391,
813 doi:10.1016/j.dsr.2010.07.009, 2010.

814 Levitus, S., Antonov, J. I., Boyer, T. P., Baranova, O. K., Garcia, H. E., Locarnini, R. A., Mishonov, A. V.,
815 Reagan, J. R., Seidov, D., Yarosh, E. S., and Zweng, M. M.: World ocean heat content and
816 thermosteric sea level change (0–2000 m), 1955–2010, *Geophysical Research Letter*, 39, L10603,
817 doi:10.1029/2012GL051106, 2012.

818 Lohmann, K., Drange, H., and Bentsen, M.: Response of the North Atlantic subpolar gyre to persistent
819 North Atlantic Oscillation like forcing, *Climate Dyn.*, 32, 273–285, doi:10.1007/s00382-008-0467-6,
820 2009.

821 Lux, M., Mercier, H., and Arhan, M.: Interhemispheric exchanges of mass and heat in the Atlantic
822 Ocean in January–March 1993, *Deep-Sea Res. Pt. I*, 48, 605–638, 2001.

823 Marsh, R., Josey, S. A., de Cuevas, B. A., Redbourn, L. J. and Quartly, G. D.: Mechanisms for recent
824 warming of the North Atlantic: Insights gained with an eddy-permitting model, *J. Geophys. Res.*, 113,
825 C04031, doi:10.1029/2007JC004096, 2008.

826 Mercier, H.: Determining the general circulation of the ocean: a non linear inverse problem, *J.*
827 *Geophys. Res.*, 91, 5103–5109, doi:10.1029/JC091iC04p05103, 1986.

828 Mercier, H., Lherminier, P., Sarafanov, A., Gaillard, F., Daniault, N., Desbruyères, D., Falina, A., Ferron,
829 B., Gourcuff, C., Huck, T., Thierry, V.: Variability of the meridional overturning circulation at the
830 Greenland–Portugal OVIDE section from 1993 to 2010, *Prog. Oceanogr.*, 132, 250–261,
831 doi:10.1016/j.pocean.2013.11.001, 2015.

832 Pérez, F. F., Mercier, H., Vázquez-Rodríguez, M., Lherminier, P., Velo, A., Pardo P. C., Rosón, G. and
833 Ríos, A. F.: Atlantic Ocean CO₂ uptake reduced by weakening of the meridional overturning
834 circulation. *Nat Geosci*, doi:10.1038/NGEO1680, 2013.

835 Pérez, F. F., Vázquez-Rodríguez, M., Mercier, H., Velo, A., Lherminier, P. and Ríos, A.F.: Trends of
836 anthropogenic CO₂ storage in North Atlantic water masses. *Biogeosciences*, 7, 1789 – 1807,
837 doi:10.5194/bg-7-1789-2010, 2010.

838 Piron, A. (2015).: *Observation de la convection profonde en mer d'Irminge sur la période 2002-2015*
839 *par les flotteurs Argo*, PhD Thesis, Université de Bretagne Occidentale.
840 <http://archimer.ifremer.fr/doc/00313/42434/>

841 Piron, A., Thierry, V., Mercier, H., and Caniaux, G.: Gyre-scale deep convection in the subpolar North
842 Atlantic Ocean during winter 2014–2015, *Geophys. Res. Lett.*, 44, 1439–1447,
843 doi:10.1002/2016GL071895, 2017.

844 Rhein, Monika., Kieke, D., Hüttl-Kabus, S., Roessler, A., Mertens, C., Meissner, R., Klein, B., Böning,
845 CW., Yashayaev, I.: Deep water formation, the subpolar gyre, and the meridional overturning
846 circulation in the subpolar North Atlantic, *Deep-Sea Research II*, 58, 1819–1832,
847 doi:10.1016/j.dsr2.2010.10.061, 2011.

848 Riser, S. C., Freeland, H. J., Roemmich, D., Wijffels, S., Troisi, A., Belbeoch, M., Gilbert, D., Xu,
849 J., Pouliquen, S., Ann, T., Le Traon, P. Y., Maze, G., Klein, B., Ravichandran M., Grant, F., Poulain, P.
850 M., Suga, T., Lim, B., Sterl, A., Sutton, P., Mork, K. A., Velez-Belch, J. P., Ansorge, I., King, B., Turton, J.,
851 Baringer, M., Jayne, S. R.: Fifteen years of ocean observations with the global Argo array. *Nature*
852 *Climate Change*, 6(2), 145–153, doi:10.1038/NCLIMATE2872, 2016.

853 Robson, J., Sutton, R., Lohmann, K., Smith, D., and Palmer, M.: Causes of the Rapid Warming of the
854 North Atlantic Ocean in the Mid-1990s, *Journal of Climate*, doi: 10.1175/JCLI-D-11-00443.1, 2012.

855 Robson, J., Sutton, R. and Smith, D.: Decadal predictions of the cooling and freshening of the North
856 Atlantic in the 1960s and the role of ocean circulation, *Clim Dyn*, 42, 2353–2365, doi:
857 10.1007/s00382-014-2115-7, 2014.

- 858 **Robson, J., Ortega, P., Sutton, R.: A reversal of climatic trends in the North Atlantic**
859 **since 2005 , *Nature Geo.*, doi: 10.1038/NGEO2727, 2016.**
- 860 **Robson, J., Polo, I., Hodson, D. L. R., Stevens, D. P., Shaffrey, L. C.: Decadal prediction of the North**
861 **Atlantic subpolar gyre in the HiGEM high-resolution climate model, *Clim. Dyn.*, DOI:**
862 **10.1007/s00382-017-3649-2, 2017.**
- 863
864 **Rossby, T., Reverdin, G., Chafik, L., and Sjøiland, H.: A direct estimate of poleward volume, heat,**
865 **and freshwater fluxes at 59.58N between Greenland and Scotland. *Journal of Geophysical***
866 **Research: Oceans, doi:10.1002/2017JC012835, 2017.**
- 867
868 *Sarafanov, A., Falina, A., Sokov, A., and Demidov, A.: Intense warming and salinification of*
869 *intermediate waters of southern origin in the eastern subpolar North Atlantic in the 1990s to mid-*
870 *2000s, *J. Geophys. Res.*, 113, C12022, doi:10.1029/2008JC004975, 2008.*
- 871 *Sarafanov, A., Falina, H., Mercier, A., Sokov, P., Lherminier, C., Gourcuff, S., Gladyshev, F., Gaillard, and*
872 *N. Daniault (2012), Mean full-depth summer circulation and transports at the northern periphery of*
873 *the Atlantic Ocean in the 2000s, *J. Geophys. Res.-Oceans*, 117(C01014), doi:10.1029/2011JC007572,*
874 *2012.*
- 875 *Sgubin G., Swingedouw D., Drijfhout S., Mary Y. and Bennabi A.: Abrupt cooling over the North*
876 *Atlantic in modern climate models, *Nature Communications* 8, 14375, doi:10.1038/ncomms14375,*
877 *2017.*
- 878 *Spall, M. A. and Price, J. F.: Mesoscale Variability in Denmark Strait: The PV Outflow Hypothesis,*
879 **Journal of Physical Oceanography*, 1997.*
- 880 *Väge, K., Pickart, R. S., Sarafanov, A., Knutsen, O., Mercier, H., Lherminier, P., van Aken, H. M.,*
881 *Meincke, J., Quadfasel, D., and Bacon, S.: The Irminger Gyre: Circulation, convection, and interannual*
882 *variability, *Deep-Sea Res. Part -Oceanogr. Res. Pap.*, 58(5), 590–614, doi:10.1016/j.dsr.2011.03.001,*
883 *2011.*
- 884 *Williams, R., Roussenov, V., Smith, D., Lozier, S.: Decadal evolution of ocean thermal anomalies in the*
885 *North Atlantic: The effects of Ekman, Overturning, and Horizontal Transport. *Journal of Climate*, 27,*
886 *doi:10.1175/JCLI-D-12-00234.1, 2014.*
- 887 *Yashayaev, I., and Loder, J. W.: Recurrent replenishment of Labrador Sea Water and associated*
888 *decadal scale variability, *J. Geophys. Res. Oceans*, 121, 8095–8114, doi:10.1002/2016JC012046, 2016.*
- 889 *Yashayaev, I., and Loder J. W.: Further intensification of deep convection in the Labrador Sea in 2016,*
890 **Geophys. Res. Lett.*, 44, 1429–1438, doi:10.1002/2016GL071668, 2017.*
- 891 *Zunino, P., Pérez, F. F., Fajar, N. M., Guallart, E. F., Ríos, A. F., Pelegrí, J. L., and Hernández-Guerra, A.:*
892 *Transports and budgets of anthropogenic CO₂ in the tropical North Atlantic in 1992–1993 and 2010–*
893 *2011, *Global Biogeochem. Cycles*, 29, 1075–1091, doi:10.1002/2014GB005075, 2015.*

894

895 **TABLES**

896 Table 1. Intensity (top-to-bottom integrated) of the different dynamical structures defined in
 897 section 3.1 for 2014 and the mean values (2002–2012) estimated by Daniault et al. (2016).
 898 **Note that the errors given for the GEOVIDE estimates come from the covariance matrix**
 899 **resulting from the inverse model. Otherwise, the errors given with the mean values are**
 900 **the standard deviation of the six estimates of each current.**

Units: Sv	WBC	IG	IC		ERRC	NAC	Recirculation
			as D2016	Northward transport			
GEOVIDE	-30.3 ± 2.1	6.8 ± 3.0	17.5 ± 7.3	22.7 ± 6.5	-13.6 ± 6.0	32.2 ± 11.4	-10.2 ± 6.4
MEAN (2002–2012)	-33.1 ± 2.6	7.7 ± 2.1	9.5 ± 3.4	11.0 ± 3.4	-12.1 ± 1.1	41.8 ± 3.7	-13.0 ± 2.0

901

902

903

904

905 **FIGURE CAPTIONS**

906 **Fig. 1.** Schematic diagram of the **2002–2012 mean** large-scale circulation adapted from
 907 Daniault et al. (2016). Bathymetry is plotted in color with color changes at 100 m, 1000 m
 908 and every 1000 m below 1000 m. The locations of the GEOVIDE hydrographic stations are
 909 indicated by black dots along the OVIDE section and across the Labrador Sea. Red dots, and
 910 associated numbers, along the OVIDE section show the stations delimiting the regions used in
 911 this paper for the transport computations **of the different currents crossing the OVIDE**
 912 **section. The names of the currents are indicated in the figure: East Greenland-Irminger**
 913 **Current (EGIC), Deep Western Boundary Current (DWBC), Irminger Current (IC),**
 914 **Eastern Reykjanes Ridge Current (ERRC), Northern branch of the North Atlantic**
 915 **Current (NNAC), Subarctic Front (SAF) and Southern branch of the North Atlantic**
 916 **Current (SNAC).** Superstations and XL stations carried out during GEOVIDE are
 917 represented by pink stars. The main topographical features of the Subpolar North Atlantic are
 918 labeled: Azores-Biscay Rise (ABR), Bight Fracture Zone (BFZ), Charlie–Gibbs Fracture
 919 Zone (CGFZ), Faraday Fracture Zone (FFZ), Maxwell Fracture Zone (MFZ), Mid-Atlantic
 920 Ridge (MAR), Iberian Abyssal Plain (IAP), Northwest Corner (NWC), Rockall Trough (RT),

921 Rockall Plateau (Rockall P.) and Maury Channel (MC). The main water masses are indicated:
922 Denmark Strait Overflow Water (DSOW), Iceland–Scotland Overflow Water (ISOW),
923 Labrador Sea Water (LSW), Mediterranean Water (MW), and Lower North East Atlantic
924 Deep Water (LNEADW).

925

926 **Fig. 2.** Vertical section of potential temperature ($^{\circ}\text{C}$), salinity and oxygen ($\mu\text{mol kg}^{-1}$) along
927 the OVIDE section measured during the GEOVIDE cruise. The horizontal grey lines in the
928 three plots represent the isopycnal layers ($\sigma_1 = 32.15 \text{ kg m}^{-3}$, $\sigma_0 = 27.80 \text{ kg m}^{-3}$ or $\sigma_2 = 36.94 \text{ kg}$
929 m^{-3} , $\sigma_4 = 45.85 \text{ kg m}^{-3}$) indicated in the upper plot. The vertical grey lines in the three plots are
930 the limits between the different circulation components crossing the OVIDE section: Western
931 Boundary Current (WBC), Irminger Gyre (IG), Irminger Current (IC), Eastern Reykjanes
932 Ridge Current (ERRC), northern branch of the North Atlantic Current (NNAC), SubArctic
933 Front (SAF), southern branch of the North Atlantic Current (SNAC) and the recirculation in
934 the Iberian Abyssal Plain (RECIR.). The main water masses are indicated in the central plot:
935 Denmark Strait Overflow Water (DSOW), Iceland–Scotland Overflow Water (ISOW),
936 Labrador Sea Water (LSW), Sub-Polar Mode Water (SPMW), Sub-Arctic Intermediate Water
937 (SAIW), North Atlantic Central Water (NACW), Mediterranean Water (MW) and North East
938 Atlantic Deep Water (NEADW). The main topographic features are indicated in the bottom
939 plot: Reykjanes Ridge (RR), Eriador Seamount (ESM), Western European Basin (WEB),
940 Azores-Biscay Rise (ABR) and Iberian Abyssal Plain (ABP). Ticks at the top of the upper and
941 central plots indicate the positions of all the stations measured during GEOVIDE, along the
942 OVIDE section, with some station numbers given above. In the bottom plot, the red and green
943 numbers indicate the position of the superstations and XLarge stations, respectively.

944

945 **Fig. 3.** Velocities (m s^{-1}) orthogonal to the OVIDE section measured during the GEOVIDE
946 cruise. Positive/negative values indicate northeastward/southwestward velocities. a)
947 Velocities measured by the ship-ADCP. b) Geostrophic velocity obtained by the inversion
948 model plus Ekman velocities in the upper 30 m. The vertical black lines are the limits between
949 the different circulation components crossing the OVIDE section as defined in the main text
950 and at the bottom of Fig. 2a. The horizontal discontinuous black line delimits the 800 dbar for
951 comparison of Fig. 3a and 3b. The horizontal black continuous lines are the isopycnals $\sigma_1 =$
952 32.15 kg m^{-3} , $\sigma_0 = 27.80 \text{ kg m}^{-3}$ or $\sigma_2 = 36.94 \text{ kg m}^{-3}$ and $\sigma_4 = 45.85 \text{ kg m}^{-3}$. Bold numbers
953 inside the figure are the volume transports (in Sv) estimated for each region and vertical layer,

954 with errors in parentheses. The only exception is the estimation of the IG transport, which,
955 following Väge et al. (2011) was computed as the northward transport (the 0 m s^{-1} isotach is
956 indicated as a thin black line in Fig. 3b in the western Irminger Sea). Station numbers at the
957 top of the figure are color-coded: black for regular stations, blue for large stations, green for
958 XLarge stations and red for superstations. The eddies described in section 3.2 are indicated at
959 the top of the plots.

960

961 **Fig. 4. Upper panel:** Stream function or volume transport horizontally accumulated from
962 Greenland to each GEOVIDE station, down to Portugal, and vertically accumulated in the
963 upper limb of the MOC (red discontinuous line) and in the whole water column (red
964 continuous line). The mean salinity in the upper limb of the MOC is also shown by the blue
965 line and labeled on the right-hand axis. Acronyms in the top of the figure indicate the different
966 components of the circulation crossing the OVIDE section as defined in Fig. 2. See Fig. 3 for
967 station numbers and bathymetry legend. **Lower panel: bathymetry along the OVIDE**
968 **section; acronyms as in Fig. 2.**

969

970 **Fig. 5.** Surface velocities (m s^{-1}) derived from AVISO data: arrows indicate current direction
971 and colors indicate current intensity. The white line represents the OVIDE section. The red
972 and ~~green~~white points indicate the extension of the different dynamical structures crossing the
973 OVIDE section in 2014. The ~~green~~white points delimit the extension of the NAC. The pink
974 stars indicate the position of the GEOVIDE superstations and XLarge stations. The
975 bathymetry contours, every 1000 m, are indicated by light ~~grey~~white lines.

976

977 **Fig. 6.** Surface velocities derived from AVISO data, as in Fig. 5, but zooming in on the NAC
978 region in March 2014, April 2014, May 2014 and June 2014. The yellow, red, clear green and
979 orange squares indicate the position of the northern, central and southern eddies, respectively,
980 discussed in section 3.2. The numbers of the GEOVIDE stations are indicated in all the plots:
981 pink for the superstations and XLarge stations, and yellow for regular stations. The red and
982 green points delimitate the position of the SAF and the NAC, respectively, at the period of the
983 GEOVIDE cruise. **The bathymetry contours, every 1000 m, are indicated by light white**
984 **lines.**

985 **Fig. 7.** Anomalies of potential temperature (upper panel, in °C), salinity (middle panel) and
986 oxygen (bottom panel, in $\mu\text{mol kg}^{-1}$) in 2014 with respect to the OVIDE 2002–2012 mean.
987 Only anomalies larger than one standard deviation of the 2002–2012 values are colored in the
988 figure. Station numbers follow the color code of Fig. 2. The orange line indicates the winter
989 mixed-layer depth (WMLD); in the Irminger Sea, the dotted line indicates the WMLD that
990 was not formed locally (see section 4.2). The acronyms in the bottom plot are as in Figs. 2 and
991 3.

992 **Fig. 8. Contours of the Absolute Dynamical Topography (ADT) averaged over 2014 (in**
993 **thin lines), contours are every 0.05 m. Thick contours correspond to the levels**
994 **encompassing the SAF front during OVIDE cruises: red for the mean 2002–2012 and**
995 **black for 2014. Note that the temporal trend on the mean ADT over the whole box (2.8**
996 **mm yr⁻¹) was removed. Bathymetry (1000 m step contours) and the OVIDE section are**
997 **plotted in white. Colors represent the absolute velocity of the current (yellow for**
998 **velocities stronger than 0.3 m s⁻¹).**

999
1000 **Fig. 9. Heat content anomalies with respect to the mean heat content for the period**
1001 **2002–2012 in the upper 1000 m of the region 40–60 °N and 45–10 °W: the monthly time**
1002 **series in grey and the 2-year running mean in black. Data source: EN4 database (Good**
1003 **et al., 2013). The red square highlights the short-term cooling event analyzed in this**
1004 **paper.**

1005
1006 **Fig. 810.** Annual mean anomalies of potential temperature (left panel) and salinity (right
1007 panel) in the surface waters (20–500 m) in the North Atlantic, estimated from ISAS database.
1008 The reference period for estimating the anomalies was 2002–2012. The OVIDE section is
1009 represented by a black line. Only anomalies larger than one standard deviation are colored in
1010 the figure.

1011
1012 **Fig. 911. 2014 Winter–Spring (DJFMAM) mean anomalies.** The anomalies were calculated in
1013 with respect the period 2002–2012. A, B and C are the total heat, sensible heat and latent heat
1014 air-sea flux, respectively, in W m^{-2} ; positive/negative values indicate ocean heat gain/lost. D,
1015 E and F are net gain of freshwater, evaporation and precipitation; the unit is 10^{-4} m;
1016 positive/negative values indicate ocean freshwater gain/loss. The contours of anomalies 0 W

1017 m^{-2} (in a, b and c) and of 0 m (in d, e and f) are represented by a white line. Data source:
1018 ERA-Interim. The green square represents the area for which the changes of heat/freshwater
1019 content, and the integrated air-sea heat/freshwater flux represented in Fig. 120 were evaluated.

1020

1021 **Fig. 120. Monthly time series of the accumulated freshwater content change between one**
1022 **month and the month before** (in m^3), **accumulated** since February 2013 in the upper 1000
1023 m of the box delimited by 40–60 °N and 45–10 °W computed from three datasets: EN4
1024 (blue), ISAS (red) and JAMSTEC (green). ~~Aaccumulated~~ **Integrated** air-sea **freshwater** flux,
1025 or precipitation minus evaporation, ~~anomalies~~ **over the same box, and accumulated from**
1026 **January 16, 2013, from ERA-Interim (continuous black line) and from NCEP**
1027 **(discontinuous black line) databases.** ~~are also plotted in black and were converted into the~~
1028 ~~same unit by repartition in the box volume; data source: ERA-Interim.~~

1029